BEACH-Domain Proteins Act together in a Cascade to Mediate Vacuolar Protein Trafficking and Disease Resistance in *Arabidopsis*

Ooi-kock Teh[a,2], Noriyuki Hatsugai[b,3], Kentaro Tamura[a], Kentaro Fuji[a,4], Ryo Tabata[c], Katsushi Yamaguchi[d], Shuji Shingenobu[d], Masashi Yamada[e], Mitsuyasu Hasebe[f,g], Shinichiro Sawa[c], Tomoo Shimada[a], and Ikuko Hara-Nishimura[a,1]

[a]Graduate School of Science, Kyoto University, Sakyo-ku, Kyoto 606-8502, Japan

[b]Research Centre for Cooperative Projects, Hokkaido University, Kita-ku, Sapporo 060-8638, Japan

[c]Graduate School of Science and Technology, Kumamoto University, Kumamoto 860-8555, Japan

[d]Functional Genomics Facility, National Institute for Basic Biology, Okazaki 444-8585, Japan

[e]Department of Biology and IGSP Center for Systems Biology, Duke University, Durham, NC 27708, USA

[f]Division of Evolutionary Biology, National Institute for Basic Biology, Okazaki 444-8585, Japan

[g]School of Life Science, The Graduate University for Advanced Studies, Okazaki 444-8585, Japan

Running title: BEACH-domain proteins of *Arabidopsis thaliana*

[1]To whom correspondence should be addressed. I. H-N. E-mail ihnishi@gr.bot.kyoto-u.ac.jp

[2]Current address: Department of Plant Biology and Forest Genetics, Uppsala BioCenter, Swedish University of Agricultural Sciences (SLU) and Linnean Centre of Plant Biology, SE-75007 Uppsala, Sweden

[3]Current address: Microbial and Plant Genomics Institute, University of Minnesota, St. Paul, MN 55108, USA

[4]Current address: RIKEN Innovation Center, RIKEN 2-1, Hirosawa, Wako, Saitama 351-0198, Japan

ABSTRACT

Membrane trafficking to the protein storage vacuole (PSV) is a specialized process in seeds plants. However, this trafficking mechanism to PSV is poorly defined. Here, we show that three types of Beige and Chediak-Higashi (BEACH)-domain proteins contribute to both vacuolar protein transport and effector-triggered immunity (ETI). We screened a green-fluorescent seed (GFS) library of *Arabidopsis* mutants with defects in vesicle trafficking and isolated two allelic mutants *gfs3* and *gfs12* with a defect in seed protein transport to PSV. The gene responsible for the phenotype was a gene encoding a protein belonging to Group D of BEACH-domain proteins, which possess kinase domains. Disruption of other BEACH-encoding loci in the *gfs12* mutant showed that BEACH homologs acted in a cascading manner for PSV trafficking. The epistatic genetic interactions observed among BEACH homologs were also reflected in the ETI responses of the *gfs12* and *gfs12 bchb-1* mutants, which showed elevated avirulent bacterial growth. The GFS12 kinase domain interacted specifically with the pleckstrin-homology domain of BchC1. These results suggest that a cascade of multiple BEACH-domain proteins contributes to vacuolar protein transport and ETI plant defence.

Keywords: BEACH domain protein; *Arabidopsis thaliana*; vacuolar protein transport; protein storage vacuoles; plant immunity.

INTRODUCTION

The cells of higher plants have two functionally distinct vacuoles (Paris et al., 1996; Neuhaus and Rogers, 1998), lytic vacuoles (LV, equivalent to lysosomes in mammals) which are found in all eukaryotic cells, and protein storage vacuoles (PSV), which are specific to higher plants and function as a storage site for storage proteins. The storage proteins constitute an essential source of amino acids for various biosynthetic activities during seed germination and also represent a major nutritional supplement for human and livestock (Okita and Rogers, 1996; North et al., 2010). Evidence for the coexistence of lytic and storage vacuoles in plant cells

came from the observation that antisera of γ-tonoplast intrinsic proteins (TIP) and α-TIP, which are markers for LV and PSV respectively, labelled vacuole membranes of two different compartments in the root tip squashes of barley and pea seedlings (Paris et al., 1996). However, the multiple-vacuole coexistence hypothesis was recently challenged by contradictory findings that fluorescently labelled γ-, α- and δ-TIP proteins localized to a common vacuolar location in *Arabidopsis* cells (Hunter et al., 2007; Frigerio et al., 2008).

Protein sorting to vacuoles with distinctive functions requires additional and specialised trafficking mechanisms. In mammalian and yeast cells, vacuolar sorting and delivery mechanisms share some fundamental features in that they are clathrin-dependent and involve interactions between the sorting receptor and AP1 adaptor complex (Ghosh et al., 2003; Nakayama and Wakatsuki, 2003). In mammalian cells, lysosomal acid hydrolases are sorted from secretory proteins at the *trans*-Golgi network (TGN) by the mannose-6-phophate receptor (MPR) (Rohrer and Kornfeld, 2001). Mannose-6-phosphate receptor-ligand complexes are then packaged into clathrin-coated vesicles, a process facilitated by the monomeric GGAs (Golgi-localized, γ-ear containing ARF-binding proteins) and the tetrameric AP1 adaptor complex (Doray et al., 2002). Similarly, carboxypeptidase Y in yeast cells is transported to the vacuoles by Vps10p, a mammalian MPR analogue, through interaction between the cytoplasmic tail of Vps10p, an AP1 adaptor complex and GGAs (Costaguta et al., 2001; Deloche et al., 2001). We have shown that *Arabidopsis* AP-1 complex may facilitate the TGN-to-cell plate trafficking of a cytokinesis-specific syntaxin, KNOLLE, during cell division (Teh et al., 2013). This highlights the imminent needs to further delineate the already complicated vacuolar sorting mechanisms at the TGN.

In plant cells the coexistence of two functionally distinct vacuoles adds a layer of complexity to the vacuolar sorting mechanisms. Soluble proteins destined for the LV requires an NPIR type sequence-specific vacuolar sorting determinant (ssVSD) in order to be recognised by the vacuolar sorting receptor BP-80, although other non-NPIR type ssVSDs have also been documented (Kirsch et al., 1994; Saalbach et al., 1996; Matsuoka and Neuhaus, 1999; Frigerio et al., 2001). In contrast to ssVSDs found in LV-targeted proteins, no consensus motifs have been identified in the PSV-targeted proteins, probably due to the sequence heterogeneity in the storage proteins studied so far (Robinson et al., 2005). Sorting signals may not be the sole determining factor for proper PSV targeting. First, some storage

proteins such as ricin and castor bean 2S albumin are also found to harbor LV-specific ssVSDs and to interact with BP-80 *in vitro* (Frigerio et al., 2001; Jolliffe et al., 2004). Second, a vacuolar sorting receptor loss-of-function mutant in *Arabidopsis*, *vsr1* (*vacuolar sorting receptor1*), missorted majority of the storage proteins to the extracellular space and a small portion of the storage proteins are still sorted normally (Shimada et al., 2003). Third, the vacuolar proteins in *vsr1* were missorted non-specifically regardless of the type of sorting signals the cargoes carried (Craddock et al., 2008). Indirect evidence has suggested that trafficking pathways to LV and PSV could operate independently since trafficking to the LV was found to be selectively inhibited while PSV targeting remained unaffected (Bolte et al., 2004; Park et al., 2005; Sanmartin et al., 2007).

An effective approach to identify key components/gene products in vacuolar trafficking is systematic genetic screening, in which mutant lines that display compromised vacuolar trafficking (e.g. accumulation of premature/unprocessed forms of vacuolar proteins) from a mutagenized population are isolated and the responsible genes mapped. However, such an approach faces two hurdles. First, most vacuolar sorting mutants display no or pleiotropic macrophenotypes (Shimada et al., 2003; Yano et al., 2003; Niihama et al., 2009; Feraru et al., 2010; Pourcher et al., 2010; Zwiewka et al., 2011), which precludes the use of forward genetic screens by growth phenotypes. Second, functional redundancy between genes of the same family complicates the analysis of single loss-of-function mutants, making it difficult to assign a gene of interest to specific trafficking roles (Sanmartin et al., 2007; Zouhar et al., 2010). In order to identify novel components involved in plant vacuolar sorting mechanisms, we previously described a high-throughput screening system that used a PSV-targeted GFP reporter (Fuji et al., 2007). The GFP reporter is fused to CT24, a PSV targeting signal from the soybean β-conglycinin, and when expressed in *Arabidopsis* seeds, GFP-CT24 is transported to the PSV (Nishizawa et al., 2003; Fuji et al., 2007). GFP-CT24 has been validated to be an efficient reporter for vacuolar sorting deficiencies since expression in *vacuolar sorting receptor1* (*vsr1*) caused GFP to be secreted and led to enhanced fluorescent in the *vsr1* seeds (Fuji et al., 2007). The enhanced fluorescent phenotype in seeds with compromised vacuolar trafficking allows rapid isolation of putative mutant lines.

Here we characterise the *green fluorescent seed12* (*gfs12)*, which is a mutant line for the Beige and Chediak-Higashi (BEACH) domain gene. The BEACH domain is a ~280

amino acid-long domain that is highly conserved in the eukaryotes (Barbosa et al., 1996). BEACH-domain containing proteins are thought to act as scaffolds to facilitate membrane events such as vesicle fusion or fission in order to regulate trafficking, although direct evidence for its mechanistic actions remains elusive (Cullinane et al., 2013). In plants, the role of BEACH-domain protein in facilitating vacuolar proteins has not been demonstrated. Using genetics and biochemistry approaches we show that members of the BEACH family proteins act together in a cascade to mediate PSV-targeted trafficking and plant immunity in *Arabidopsis*.

RESULTS

GFS12 Encodes a BEACH-Domain Protein

The *gfs12* mutant was isolated for its enhanced GFP fluorescence in the seeds when compared to the parental line GFP-CT24 (Figure 1A). The enhanced GFP fluorescence in *gfs12* indicated that the PSV-targeted GFP was mis-sorted to intercellular space and implied that trafficking to the PSV is compromised. The *GFS12* mutation is recessive and segregated in a simple Mendelian manner. *gfs12* displayed no obvious growth defects throughout the life cycle. Unlike *vsr1*, which has previously been shown to abnormally accumulated the unprocessed precursor forms of two major PSV proteins 2S albumins and 12S globulins (Shimada et al., 2003; Fuji et al., 2007), *gfs12* seeds accumulated predominantly the 12S globulins precursor (p12S) and trace amount of the 2S albumins precursor (p2S) when analysed on immunoblotting (Figure 1B). Since the accumulation of unprocessed 12S globulin is the predominant phenotype in *gfs12*, we decided to focus on this phenotype in the subsequent analysis.

Map-based cloning and whole genome sequencing of *gfs12* identified a G-to-A transition at the 966th nucleotide in locus At5g18525, which encodes a protein with a Beige and Chediak-Higashi (BEACH) domain (Figure 2A). The BEACH domain is named after a rare autosomal genetic disorder called Chediak-Higashi syndrome (Barbosa et al., 1996) and defines a large family of genes that are conserved across all eukaryotes. The BEACH domain proteins are usually very large in size and share a similar structural organisation (Figure 2A).

Though the function of the BEACH domain is unknown, BEACH domain proteins have been implicated in diverse cellular processes such as vesicle trafficking, cytokinesis and receptor signalling (Kwak et al., 1999; Su et al., 2004; Khodosh et al., 2006). For the ease of discussion, we subsequently renamed the At5g18525 locus as *GFS12*. *GFS12* encodes a 1637 amino acid polypeptide with two putative kinase domains flanking the 232-amino acid long BEACH domain. Like all other BEACH proteins, the extreme C-terminus of GFS12 harbors the highly conserved WD40 repeats which have regulatory roles and are involved in protein-protein interactions (Neer et al., 1994). The EMS-induced G-to-A transition in *GFS12* replaced the 322th tryptophan codon with a stop codon and created a premature termination before the BEACH domain (Figure 2A). We subsequently identified an additional *GFS12* allele from the same genetics screen, *gfs3* which has a Trp-1239-stop nonsense point mutation in *GFS12* (Figure 2A). *gfs3* was therefore renamed as *gfs12-2*. *gfs12-2* shared the p12S accumulation phenotype as *gfs12* (Figures 1B). Both *gfs12* and *gfs12-2* were null alleles as we were unable to detect *GFS12* transcripts in the RT-PCR analyses (Figure 2B). To confirm that the point mutations in the *gfs12* mutants were indeed responsible for the p12S accumulation phenotype, we transformed *gsf12* and *gfs12-2* plants with a 35S promoter-driven GFS12-RFP (red fluorescent protein) fusion protein and showed that the phenotype was complemented by an exogenous wild-type copy of *GFS12* (Figure 2C and Supplemental Figure 1). This provides direct evidence that the disruption of *GFS12* caused the p12S accumulation in *gfs12* mutants and that the GFS12-RFP fusion protein is functional.

The p12S accumulation in *gfs12* seems to be a highly specific trafficking defect that is found in the seeds but not in vacuolated vegetative tissues. Stable expression of the secretory marker secRFP (Zheng et al., 2004) and the tonoplast marker GFP-ɣ-TIP (Hunter et al., 2007) in *gfs12* showed that these marker proteins were correctly trafficked to the intercellular space and vacuolar membrane, respectively (Supplemental Figure 2A-2D). Thereore, defects in the membrane trafficking of these fluorescent markers in vegetative cells were not detected.

We next investigated the tissue expression pattern of *GFS12* using a promoter-GUS fusion gene (*GFS12*$_{pro}$*:GUS*). In *Arabidopsis* plants expressing *GFS12*$_{pro}$*:GUS*, GUS activities were weakly found in the cotyledons of germinating seedlings (Supplemental Figure 3A). GUS-staining showed that *GFS12* expression was restricted to the vasculature tissues of cotyledons and root tissues. *GFS12* was also expressed at the apical meristem, root tip, young

flower buds, and receptacles (Supplemental Figure 3).

The *Arabidopsis* BEACH-Domain Proteins Can Be Classified into Four Groups

The *Arabidopsis* genome contains six BEACH domain-containing genes, namely *GFS12* (At5g18525), *SPIRRIG* (At1g03060), At4g02660, At1g58230, At2g45540 and At3g60920 (Saedler et al., 2009). Only one of these genes, *SPIRRIG* (At1g03060), has been characterised so far. The *SPIRRIG* gene has a role in cell morphogenesis as the *sprrig* (*spi*) mutant displayed pleiotropic cellular distortion. Vacuoles in *spi* root hairs, like PSV in *gfs12* seeds, are highly fragmented (Saedler et al., 2009). In a phylogenetic tree of BEACH-domain proteins (Supplemental Table 1), *Arabidopsis* BEACH proteins fell into four groups, A, B, C and D (Figure 3). At3g60920 and At2g45540 were in Group C, while At4g02660 and SPIRRIG/At1g03060 were in Group A. The tree shows that the GFS12/BchD diverged from other mammalian and yeast BEACH proteins to form an outgroup that is characterised by plant-specific BEACH proteins with kinase domains (Supplemental Figure 4), suggesting this group of BEACH protein has evolved to acquire plant-specific functions (Figure 3, Group D). Moreover the bootstrap value of 70 for the Group D provides additional evidence for the outbranching of the group (Figure 3). Interestingly, GFS12 is the only *Arabidopsis* BEACH protein that possesses kinase domains that flank the BEACH domain (Figure 4A). A phylogenetic analysis based on the PH-BEACH-WD40 domains arrived at a similar conclusion (Saedler et al., 2009), although At3g60920 was not included in the analysis because it lacks the WD40 repeats.

Genetic Interactions between *GFS12* and BEACH Homologs

We next investigated the possible involvement of BEACH protein homologs in PSV sorting. To this end, we isolated T-DNA knock-out or knock-down mutants (Supplemental Figure 5) from every BEACH domain-encoding gene in *Arabidopsis* and analysed the seed protein profiles. In summary, while *gfs12* accumulated p12S (Figure 4B), none of the mutant alleles of *AtBchA1*, *AtbchA2*, *AtBchC1* and *AtBchC2* accumulated either p12S or p2S. One allele from the *AtBchB*, *bchb-1* weakly accumulated p12S only (Figure 4B).

We further examined the possible genetic interactions between *GFS12/BchD* and other BEACH protein homologs. We therefore selected one representative BEACH member from Groups B and C to generate double mutants *gfs12 bchb-1* and *gfs12 bchc1-1*. We found that p12S accumulation by the double mutant *gfs12 bchb-1* was greatly enhanced and similar to that in *vsr1-2* (Figure 5A). Accordingly p2S also began to highly accumulate in *gfs12 bchb-1*, a phenotype which was not observed in the *gfs12*, indicating that AtBchB functionally overlaps with GFS12/BchD to mediate 12S globulins and 2S albumins trafficking to the PSV (Figure 5A). Surprisingly, knocking out *AtBchC1* in *gfs12* rescued the p12S accumulation, as the *gfs12 bchc1-1* double mutant no longer accumulated the p12S (Figure 5A). The genetic suppression observed in the *gfs12 bchc1-1* double mutant indicates that AtBchC1 plays an epistatic role to GFS12. The absence of p12S in seeds of the *bchc1-1* single mutant (Figure 4B) suggests that *BchC1* acts downstream of *GFS12* at the PSV-targeted trafficking. Therefore the most likely explanation for the suppression phenotype in *gfs12 bchc1-1* would be that GFS12/BchD acts to inhibit BchC1, which is a negative regulator of PSV-targeted trafficking (see Figure 8).

The overlapping/redundant function between GFS12/BchD and BchB prompted us to ask the question whether BchB acts independently or through inhibiting the BchC1 to mediate PSV trafficking. To distinguish these two possibilities genetically, we examined the level of p12S and p2S accumulation in the seeds of triple mutant *gfs12 bchb-1 bchc1-1*. The enhanced p12S and p2S accumulations seen in the double mutant *gfs12 bchb-1* were greatly or totally eliminated, respectively by the *bchc1-1* mutation (Figure 5A), indicating that BchB functions in parallel with the GFS12/BchD to inhibit the BchC1 (see Figure 8). Surprisingly, the BEACH homologs do not seem to be essential for the general plant growth as mutants of all combinatorial mutations displayed normal development throughout their life cycle (Figure 5B).

The GFS12/BchD Kinase Domain Physically Interacts with specific sites of the Pleckstrin Homology Domain of BchC1

The BchB and BchC1 proteins each possesses a pleckstrin homology (PH) domain, which is known to physically interact with a wide range of signalling molecules such as

phosphoinositols and kinases to facilitate membrane targeting and trafficking (Yao et al., 1994; Lemmon, 2004). Since GFS12/BchD is characterised by two kinase domains, we therefore ask the question does the kinase and BEACH domains in GFS12/BchD interact with BchB and/or BchC1 PH domains. Using the yeast two hybrid assay, we examined the interaction between N-terminal kinase domain I (K1), C-terminal kinase domain II (K2) and BEACH domain (Bch) of GFS12/BchD with PH domains of BchB (B PH-Bch) and BchC1 (C1 PH-Bch) (Figure 4A). All yeast strains harboring the bait/prey empty vectors did not show auto-activation when transformed with the designated bait/prey proteins (Figure 6A, top most and left most panels). The GFS12/BchD K1, K2 and Bch proteins have no detectable interaction amongst themselves (Figure 6A). We further tested all the possible combinations of bait and prey proteins between GFS12/BchD, BchB and BchC1 and only interaction between K2 and C1 PH-Bch was detected (Figure 6A). We confirmed this interaction by swapping the prey and bait cloning vector between K2 and C1 PH-Bch (Supplemental Figure 6).

Previously the crystal structure of a human BEACH homolog Neurobeachin (Nbea) has been determined at the 2.9 Å resolution (Jogl et al., 2002). The Nbea PH domain is able to interact with its own BEACH domain via an extensive interface. This interaction is highly dependent on the conserved amino acid residues distributed in the PH and BEACH domains (Jogl et al., 2002). To clarify a specific interaction between the GFS12/BchD K2 and BchC1 PH-Bch domains, we introduced mutations at two highly conserved amino acids each in the PH and BEACH domains of BchC1. When R1615E (corresponds to R2208 in Nbea) and E1625R (corresponds to E2218 in Nbea) mutations were introduced in the BchC1 PH domain, the interaction between GFS12/BchD K2 and C1 PH-Bch was abolished (Figure 6B). On the contrary, the interaction remained unchanged in the N1704A (corresponds to N2302 in Nbea) and Q1708A (corresponds Q2306 in Nbea) BEACH mutants (Figure 6B). We therefore concluded that the R1615 and E1625 amino acids in the BchC1 PH domain are crucial for the physical interaction with K2 domain of GFS12/BchD.

GFS12/BchD and BEACH Proteins Are Required for Effector-Triggered Immunity

Endosomal trafficking components have recently been implicated in the plant immunity

response upon pathogenesis (Beck et al., 2012; Uemura et al., 2012). Therefore we investigated the possible involvement of BEACH proteins in mediating effector-triggered immunity (ETI) induced by *Pseudomonas syringae* pv. *tomato* (*Pst*DC3000/*avrRpm1*). In control CT24 parental plants, growth of the avirulent bacteria was 10^4 cfu/ml, whereas it was two orders of magnitude higher in *gfs12* (10^6 cfu/ml, Figure 7A). The compromised immune response in *gfs12* was GFS12-dependent, as a proper ETI response was restored in the complemented *gfs12* lines (Figure 7B). Analysis of the ETI response in double mutants of BEACH homologues revealed an interesting correlation with the PSV trafficking defects described earlier. In *gfs12 bchc1-1*, in which p12S accumulation was suppressed, the compromised ETI response was also inhibited and exhibited the same bacterial titre as the control parental plants (Figure 7A). On the other hand, *gfs12 bchb-1* showed a severed ETI response (bacterial growth titre 10^6 cfu/ml. Figure 7A), which correlates well with the enhanced p12S and p2S accumulation phenotype.

To further delineate the involvement of BEACH domain proteins in ETI, we examined the ETI-associated hypersensitive cell death in *gfs12* by ion leakage assay upon inoculation with *Pst*DC3000/*avrRpm1*. The ion leakage assay in which *gfs12*, *gfs12 bchc1-1*, *gfs12 bchb-1* and the complemented *gfs12* showed elevated conductance, similar to that in the control parental plants, indicating that all the BEACH mutants were able to initiate hypersensitive cell death (Figure 7C). We therefore concluded that the BEACH proteins play an essential role in ETI but not in the cell death.

DISCUSSION

Since the identification of the first BEACH-domain containing protein in 1996, the protein family represents an enigmatic class of trafficking-related protein with elusive functions (Barbosa et al., 1996). Extensive characterization of the mammalian BEACH homolog Lysosomal Trafficking Regulator (LYST) has revealed a role in the neuronal cell lysosomal trafficking, however the mechanisms and functional role of the BEACH domain in mediating lysosomal trafficking are still poorly defined (Wang et al., 2000; de Souza et al., 2007; Lim and Kraut, 2009). BEACH proteins have a large size (>400 kDa) which makes

characterization difficult and therefore the subcellular localization of the BEACH homologs has been elusive. Although BEACH proteins do not have transmembrane domains, subcellular fractionation of the yeast BEACH homolog, Beige Protein Homologue 1, suggests that it is a membrane-associated protein (Shiflett et al., 2004). In an immunolocalization experiment, the mammalian BEACH homolog Neurobeachin was shown to label unidentified polymorphic tubulovesicular endomembranes (Wang et al., 2000). The *Dictyostelium* and *Drosophila* BEACH homologs are lysosome-associated, which indicates that they have roles in lysosomal trafficking (Kypri et al., 2007; Lim and Kraut, 2009). Whether these differential localizations between the BEACH homologs represent their functional divergence or a novel cellular compartment specific to the BEACH protein remain to be determined.

The epistatic genetic interactions observed between GFS12/BchD, BchB and BchC1 highlight the hierarchical/cascading actions of the BEACH homologs in negatively mediating PSV trafficking and plant ETI (Figure 8). We propose that GFS12/BchD acts predominantly to suppress BchC1, which itself is a negative factor in PSV trafficking regulation and plant immunity response (Figure 8). Furthermore, the additive effects of *bchb-1* mutation on the PSV trafficking phenotype in *gfs12-1* (Figure 5) is a strong indication that GFS12 and BchB act to suppress BchC1. Multiple independent traffikcing pathways to vacuoles have recently been described (Ebine et al., 2014; Singh et al., 2014). Although our genetic analysis and our yeast two hybrid analysis (see below) support the proposed working model, we cannot rule out the possibility that BchC1 might act as an negative regulator of an entirely independent PSV trafficking pathway where elimination of BchC1 results in bypassing the GFS12- and BchB-dependent pathway.

Our yeast two hybrid analysis (Figure 6) shows that Kinase II domain (K2) of GFS12/BchD specifically interacts with the BchC1 PH domain. Based on this interaction, we propose a working model of the inhibitory effects of BEACH proteins on PSV trafficking and plant immunity response (Figure 8). In this working model, the GFS12/BchD Kinase II domain phosphorylates BchC1 via protein-protein interaction mediated by the PH domain in BchC1. Phosphorylation of BchC1 by the GFS12/BchD will induce conformational changes in BchC1 that will inactivate it. Further studies using X-ray crystallography on the phosphorylated of BchC1 upon phosphorylation is necessary to prove the case. Our working model also implies that the expression level of BchC1, a negative regulator, should be kept at

the lowest to ensure PSV trafficking and immunity response is minimally inhibited. In consistent with this, the mean expression levels of BchC1 is the lowest compared to that of GFS12/BchD and BchB (Supplemental Figure 7) (Obayashi et al., 2011). The relatively higher expression levels of the GFS12/BchD and BchB compared to the BchC1 would ensure that the inhibitory effects of BchC1 are kept in check.

Interestingly, all three BEACH proteins characterised in this study exert inhibitory effects in a cascade to fine tune PSV trafficking as shown in Figure 8. Notably, BEACH homologs from other model organisms seem to have similar regulatory effects. For example, the *Dictyostelium* LvsB and *Drosophila* MAUVE (a LYST homolog) act as negative regulators to limit the homotypic and heterotypic fusions of early endosomes with postlysosomal compartments (Kypri et al., 2007; Rahman et al., 2012); a *C. elegans* BEACH homolog, SEL-2 (a neurobeachin homolog), negatively regulates the Notch activity in polarised epithelial cells (de Souza et al., 2007) and finally the *Drosophila* Blue Cheese antagonises the small GTPase Rab11 during synapse morphogenesis (Khodosh et al., 2006). These findings exemplified a common feature of the BEACH proteins: they are the negative regulators of lysosomal trafficking.

All BEACH mutants reported so far share a diagnostic phenotype which is an enlarged lysosome (Introne et al., 1999). This mutant phenotype has led to the suggestion that BEACH proteins function to limit the homotypic fusions of the lysosomal compartments. The lysosome equivalent in plants is the lytic vacuole. Using the vacuolar membrane marker GFP-ɣ-TIP, we confirmed that the morphology of the lytic vacuole remained unchanged in the *gfs12* mutant (Supplemental Figure 2C and 2D).

Interestingly, the compromised ETI phenotypes of *gfs12 bchc1-1* and *gfs12 bchb-1* correlate well with the PSV trafficking defects in these mutants. This observation is unexpected, since the *gfs12* and *bchb-1* mutations only impacted on storage protein trafficking in seeds while no other discernible trafficking defects was observed in mature rosette leaves where ETI takes place. A possible explanation for this unexpected observation would be that the ubiquitously-expressed BEACH-related proteins GFS12 and BchB (Supplemental Figure 7) function at PSV trafficking in embryos and defence-associated trafficking in rosette leaves. In support of this, mounting evidence showed that membrane trafficking proteins play substantial roles in plant immunity (Teh and Hofius, 2014). It is also interesting to note that

although *gfs12 bchb-1* showed compromised ETI, avrRpm1-conditioned HR-cell death was not affected, implying that GFS12 and BchB act specifically in ETI which could be uncoupled with the HR cell death (Heidrich et al., 2011; Teh and Hofius, 2014).

In conclusion, the data presented here demonstrated that *Arabidopsis* BEACH proteins are multifunctional proteins that are required for PSV trafficking and plant immunity. By acting in a cascade manner, the BEACH proteins form a hierarchy network that helps to fine tune PSV trafficking during seed development. Further delineation of the protein functions would require substantial knowledge on the subcellular localization of the BEACH proteins as well as careful dissection of the conserved BEACH domains.

METHODS

Plant Materials and Growth Conditions

Arabidopsis T-DNA insertion lines were obtained from the Arabidopsis Biological Resource Center. A list detailing all lines used in this study is described in the supplemental information.

Mapping and Next Generation Sequencing

The *gfs12* mutations were roughly mapped to a 200-kb region on chromosome 5, and the genomic DNA was analysed by next generation sequencing as described in (Tabata et al., 2012) to identify the mutations.

Arabidopsis Complementation

A genomic full-length fragment of *GFS12* was amplified using primers GFS12-infusion-F (5’ aaccaattcagtcgacatgagaggtgaagatagtgacctttgc3’) and GFS12-infusion-CR (5’aagctgggtctagatatccacaacagattctcaagtgaccatcatg3’). The fragment was cloned into entry vector pENTR1A (Invitrogen) using an In-Fusion Cloning Kit (Clontech). To generate $35S_{pro}$:GFS12-RFP, the GFS12 genomic fragment was subcloned to pGWB560 by Gateway® LR reactions. A complementation experiment was carried out by transforming the *gfs12* plants with $35S_{pro}$:GFS12-RFP using the floral dip method; primary transformants were selected on hygromycin-containing MS media and propagated to T3 generations in order to obtain

homozygous lines. To generate a GUS reporter line for the GFS12 promoter, a 2-kb genomic fragment upstream of the GFS12 start codon was amplified using primers pGFS12-infusion-F (5'aaccaattcagtcgacacgcagatatgagcgacggaatcc3') and pGFS12-infusion-R (5'aagctgggtctagatatccccccttctttcttggaggaagagag3'). The PCR fragment was cloned into pENTR1A by an In-Fusion cloning kit and further sublconed to pHGWFS7 to generate $GFS12_{pro}$:EGFP-GUS.

GUS Staining and Drug Treatment

Seedlings and tissues of transgenic lines harboring $GFS12_{pro}$:EGFP-GUS were incubated on ice in cold 90% acetone for 15 min, vacuum infiltrated for 15 min in the GUS staining solution (0.5 mg/ml X-Gluc, 100 mM NaH_2PO4, 10 mM EDTA, 0.1% Triton X-100, 5 mM $K_4[Fe(CN)_6]$) to improve its penetration into tissues, incubated overnight at 37°C in the staining solution, transferred to 70% ethanol and destained in ethanol: acetic acid (6:1) with gentle shaking. Four to 5-day old seedlings were used for confocal imaging experiments. For FM4-64 (an endocytic tracer that labels endosomes) staining, seedlings were incubated in 5 µM FM4-64 for 5 min at room temperatures and washed briefly in sterile water before proceeding to imaging. To visualise BFA compartments (agglomerations of endosomes and *trans*-Golgi network due to BFA treatment), seedlings were pre-stained with FM4-64 before incubating in 50 µM BFA solution for 1 h.

SDS-PAGE and Immunoblots

Seed proteins were extracted from a pool of 50 seeds in 50 µl of extraction buffer [50 mM Tris-HCl (pH6.8), 250 mM NaCl, 25 mM EDTA, 50%v/v glycerol, 0.5% v/v 2-mercaptoethanol, 1% v/v SDS]. Proteins from 5-8 seeds was analysed on SDS-PAGE. 12S globulin and 2S albumin were immunodetected with rabbit anti-12S and anti-2S antibodies at 10,000 x and 5,000 x dilutions.

Pathogen Strains, Pathogen Tests and Evaluation of Cell Death

The avirulent bacterial strain *Pseudomonas syringae* pv. tomato DC3000/*avrRpm1* (*Pst*DC3000/*avrRpm1*) was used in this study. Leaves were infiltrated with freshly cultured *Pst*DC3000/*avrRpm1* as described previously (Hatsugai et al., 2009). Plant immunity and cell death caused by *Pst*DC3000/*avrRpm1* were assayed by measuring the bacterial growth and

ion leakage, respectively (Hatsugai et al., 2009).

Yeast-Two-Hybrid Assay

Yeast strain AH109, expression cassettes pDEST-GADT7 (Rossignol et al., 2007) and pDEST-GBKT7 (Rossignol et al., 2007) were used throughout this study. cDNA of specific domains from GFS12, BchB and BchC1 were amplified by PCR (Supplemental Table 2), sequenced and cloned into the expression cassettes by Gateway cloning. To co-transform the yeast strain AH109, a 100 mL culture (subcultured from an overnight culture) was grown to OD_{600} 0.5, centrifuged at 1500 x *g* for 5 min, washed in distilled water and resuspended in 1 mL 0.1 M Lithium acetate/TE buffer. Twenty-five µL of yeast suspension cells were aliquoted for each transformation. Five µL sonicated salmon sperm carrier DNA (2.5 mg/mL), 1 µg of each plasmid DNA and 200 µL PEG-4000 (50% w/v) were added to the cells in that order. The mixture was vortexed vigorously and incubated at room temperature for 1 h. The cells were by heat shock at 42^{o}C for 1 h, washed once in 800 µL distilled water, plated in SD-W-L media and grown for 3 days to select for yeast strains that harbor both expression cassettes. To test for protein-protein interaction, yeast strains co-expressing bait and prey proteins were plated on SD-W-L-H-A media for 4 days.

Supplemental Data

The following materials are available in the online version of this article.

Supplemental Figure 1. Abnormal accumulation of 12S globulin precursor (p12S) in *gfs12-2/gfs3* is complemented by a RFP-fusion protein of GFS12.

Supplemental Figure 2. Secretory and Lytic Vacuole Trafficking Pathways Were Unaffected in *gfs12*.

Supplemental Figure 3. *GFS12* Expressed Weakly in Specific Tissues.

Supplemental Figure 4. Schematic Representations of the BEACH Protein Structure.

Supplemental Figure 5. RT-PCR to Isolate Knock-Out and Knock-Down Alleles of BEACH-Domain T-DNA Mutants.

Supplemental Figure 6. Yeast-Two-Hybrid Assay of GFS12 and BchC1.

Supplemental Figure 7. Expression Levels of *GFS12*/*BchD, BchB* and *BchC1* as Indicated on the ATTED-II.

Supplemental Table 1. BEACH-Domain Amino Acid Sequences Used in the Phylogenetic

Analyses.

Supplemental Table 2. DNA Sequence of Primers Used in the RT-PCR of BEACH-Domain T-DNA Mutants and Yeast-Two-Hybrid Assay.

FUNDING

This work was supported by Specially Promoted Research of Grant-in-Aid for Scientific Research to I.H-.N. (no. 22000014) from the Japan Society for the Promotion of Science (JSPS). O-K.T. is a postdoctoral fellow under the JSPS Science Foreign Researcher Programme (no. 22-00088).

ACKNOWLEDGEMENTS

We thank Dr. Sota Fujii (Kyoto University) for advice on phylogeny analysis.

Figure Legends

Figure 1. *gfs12* and *gfs3* Are Vacuolar Protein Trafficking Mutants.

(**A**) Comparison of fluorescence of *gfs3*, *gfs12* and parental CT24 seeds expressed a PSV-targeted GFP. Imaging parameters were the same for each panel. Bars=1cm.

(**B**) 12S globulin and 2S albumin immunoblot of *gfs12* and *gfs3*. Storage protein analysis of *gfs12* and *gfs3* showed that they accumulated unprocessed 12S globulin precursors (p12S) and trace amount of unprocessed 2S albumin precursors (p2S), unlike the *vsr1-2* which massively accumulates both type of precursors.

Figure 2. *gfs12* and *gfs3* Are alleles of a BEACH-Domain Locus.

(**A**) (Top) Schematic representation of locus At5g18525. The locus is now renamed as *GFS12*. Exons and introns are indicated by boxes and lines respectively. Red arrows indicate primers used in RT-PCR. Locations of mutations in *gfs12* (G966A, W322stop) and *gfs12-2* (G3746A, W1249stop) are shown. (Bottom) Schematic representation of the corresponding *GFS12* protein structure. Kinase domains are marked by yellow ovals, blue rectangle represents BEACH domain and red oval indicates WD40 repeats.

(**B**) *gfs12* and *gfs12-2* are knock-out alleles of *GFS12*. RT-PCR of *GFS12* transcript in *gfs12* and *gfs12-2*/*gfs3*. *Actin2* was used as loading control. Primers used (F15 and R3) are indicated by red arrows in (**A**). Cycle numbers for GFS12 and Actin2 are 35 and 28 respectively.

(**C**) Abnormal accumulation of 12S globulin precursor (p12S) is complemented by a RFP-fusion protein of GFS12. Numbers on top indicate independent T3 lines of *gfs12* transformed with GFS12-RFP under 35S promoter.

Figure 3. Phylogenetic Tree of BEACH-Domain Proteins Constructed by the Neighbor-Joining Method with Phylogeny.

Amino acid sequences of the BEACH domains (Table S1) from dicot, monocot, animals, slime mould, moss, green alga and lycophyte were edited, aligned and analyzed using neighbour-joining method (Dereeper et al., 2008). GenBank accession numbers (in the case of *Arabidopsis*, AGI codes) are shown in parentheses. Green boxes indicate plant-specific BEACH homologs. Numbers at the branches indicate bootstrap values.

Figure 4. GFS12 Has Overlapping Functions with BchB in Vacuolar Protein Trafficking.

(**A**) Schematic representation of four groups of BEACH-domain protein in *Arabidopsis*. Solid line and red-filled oval represent the highly variable regions and WD40 repeat domain respectively. PH is pleckstrin homology domains. GFS12 is the only BEACH protein that possesses kinase domains. Note that WD40 repeats are missing from BchC1.

(**B**) Anti-12S and anti-2S immunoblots of BEACH homolog knock-out or knock-down mutants showing that only *gfs12* and *bchb-1* specifically accumulated 12S globulin precursor (p12S) but not 2S albumin precursors (p2S).

Figure 5. Epistatic and Synergistic Genetic Interactions between GFS12 and BEACH Homologs.

(**A**) Anti-12S and anti-2S immunoblots of BEACH-domain double mutants. GFS12 showed synergistic genetic interactions with *BchB* as double mutant *gfs12 bchb-1* accumulated significant amount of 12S globulin precursor (p12S) compared to single mutants *gfs12* and *bchb-1*. The 2S albumin precursors (p2S) also began to accumulate in *gfs12 bchb-1*. The *bchc1-1* mutation is epistatic to *gfs12* since no p12S can be detected in double mutant *gfs12 bchc1-1*. Triple mutant *gfs12 bchb-1 bchc1-1* showed reduced p12S accumulation compared to double mutant *gfs12 bchb-1*. Note that p2S accumulation in *gfs12 bchb-1* was also suppressed when *bchc1-1* mutation was introduced.

(**B**) GFS12 and BEACH homologs are not important for *Arabidopsis* general growth. All mutant combination showed normal growth compared to wild type control. Bar=1cm.

Figure 6. Yeast-Two-Hybrid Assay of GFS12, BchB and BchC1.

(**A**) The GFS12/BchD Kinase I-BEACH (GFS12/D K1-Bch), BEACH-Kinase domain II (GFS12/D Bch-K2), Kinase domain I only (GFS12/D K1), Kinase domain II only (GFS12/D K2), BEACH domain only (GFS12/D Bch), BchC1 PH-BEACH domain (C1 PH-Bch) and BchB PH-BEACH domain (B PH-Bch) were cloned in pDEST-GADT7. These constructs were tested for interaction against the bait constructs in pDEST-GBKT7 which includes C1 PH-Bch, B PH-Bch, GFS12/D K1-Bch and GFS12/D Bch-K2. Yeast strains harboring the prey and bait constructs were selected on single dropout (SD) media minus tryptophan and leucine (SD-W-L). When these yeast strains were plated on SD media without essential amino

acids histidine and adenine (SD-W-L-H-A), only yeast strain harboring pDEST-GADT7:GFS12/D K2 and pDEST-GBKT7:C1 PH-Bch grew.

(B) Site directed mutagenesis in the BchC1 PH domain (R1625E and E1625R) disrupted the BchC1 interaction with GFS12 Kinase II domain. On the contrary, mutations (N1704A and Q1708A) in the BchC1 BEACH domain have no effect on the BchC1-GFS12 Kinase II interaction.

Figure 7. Effector Triggered Immunity Is Compromised in *gfs12*.

(**A, B**) Five-week-old plants of various genetic backgrounds were infiltrated with *Pst*DC3000/*avrRpm1*. Bacterial growth titer was assayed 3 days later. Error bars=standard errors.

(**C**) Ion leakage assay of the control CT24 parental plants, *gfs12*, *gfs12 bchc1-1*, *gfs12 bchb-1* and complemented *gfs12* plants. They were infected with *Pst*DC3000/*avrRpm1*. The ion leakage from dying and dead cells was measured by conductance.

Figure 8. Working Model on the BEACH Protein Cascade Action in Regulating Storage Protein Trafficking and Plant Immunity Response.

We propose that GFS12, BchB and BchC1 acts in a cascading manner to regulate storage protein trafficking. GFS12 interacts with BchC1 via the PH domain. The interaction inactivates BchC1 which is a negative regulator for the PSV trafficking and plant immunity response. Note that GFS12 has a predominant role over BchB in BchC1 inhibition.

Supplemental information

Supplemental Figure 1. Abnormal accumulation of 12S globulin precursor (p12S) in *gfs12-2/gfs3* is complemented by a RFP-fusion protein of GFS12. Numbers on top indicate independent T3 lines of *gfs12-2/gfs3* transformed with GFS12-RFP under 35S promoter.

Supplemental Figure 2. Secretory and Lytic Vacuole Trafficking Pathways Were Unaffected in *gfs12*.

CLSM analysis of *gfs12* stably expressing different markers in cotyledon. Bars=5μm.

(A, B) Expression of the secretory marker secRFP in CT24 **(A)** and *gfs12* **(B)** showed that the secretion in *gfs12* was unaffected as RFP signal was detected in the apoplastic regions.

(C, D) Expression of vacuolar membrane protein GFP-ɣ-TIP in CT24 **(C)** and *gfs12* **(D)** showed that the membrane protein was correctly targeted to the lytic vacuole.

(E, F) BFA treatment of CT24 **(E)** and *gfs12* **(F)** stably expressing Golgi marker ST-GFP (green) showed indistinguishable phenotypes between CT24 and *gfs12*. Magenta signal was endocytic tracer FM4-64.

Supplemental Figure 3. *GFS12* Expressed Weakly in Specific Tissues.

GFS12 expression pattern as revealed by the GFS12 promoter GUS fusion. GFS12 expresses weakly from early stage of the seedling development **(A)** with distinct root tip **(D)** and vein tissues **(B)** staining pattern. High expression was also found in the apical meristem **(B, C)**. GFS12 expression was relatively weak at the reproductive stage **(E-H)**. In developing siliques, the GFS12 expression diminished as the seeds developed **(E)**. Weak expression of GFS12 was also detected in the stigma and style **(F)**, receptacles **(G)** and young flower buds **(H)**. Bars, 0.1 cm.

Supplemental Figure 4. Schematic Representations of the BEACH Protein Structure.

Kinase domains are marked by yellow ovals, blue and green rectangles represent BEACH and PH domains respectively and red oval indicates WD40 repeats. Length of proteins is not drawn to scale.

Supplemental Figure 5. RT-PCR to Isolate Knock-Out and Knock-Down Alleles of BEACH-Domain T-DNA Mutants.

Schematic representation of the T-DNA insertion (inverted triangles) in the BEACH-domain containing genes are indicated on the right and the RT-PCR analyses of the respective mutant alleles are on the left. *Actin2* was used as loading control in all cases. Darkened rectangle boxes represent exons and introns are indicated by joining lines. Primers used in the RT-PCR were indicated by arrows.

Supplemental Figure 6. Yeast-Two-Hybrid Assay of GFS12 and BchC1.

KII domain of GFS12 and PH-BCH domain of BchC1 was expressed in the bait (pDEST-GBDKT7) and prey vectors (pDEST-GADT7) respectively and grown on either SD-W-L media (bottom) or SD-W-L-H-A media (top). Self-activation negative control was also included. Only yeast strain harboring the pDEST-GBDKT7: GFS12/D K2 and pDEST-GADT7:C1 PH-BCH grew on SD-W-L-H-A media.

Supplemental Figure 7. Expression Levels of *GFS12*/*BchD*, *BchB* and *BchC1* as Indicated on the ATTED-II.

Supplemental Table 1. BEACH-Domain Amino Acid Sequences Used in the Phylogenetic Analyses.

Supplemental Table 2. DNA Sequence of Primers Used in the RT-PCR of BEACH-Domain T-DNA Mutants and Yeast-Two-Hybrid Assay.

REFERENCES

Barbosa, M.D., Nguyen, Q.A., Tchernev, V.T., Ashley, J.A., Detter, J.C., Blaydes, S.M., Brandt, S.J., Chotai, D., Hodgman, C., Solari, R.C., Lovett, M., and Kingsmore, S.F. (1996). Identification of the homologous beige and Chediak-Higashi syndrome genes. Nature. **382,** 262-265.

Beck, M., Heard, W., Mbengue, M., and Robatzek, S. (2012). The INs and OUTs of pattern recognition receptors at the cell surface. Curr. Opin. Plant Biol. **15,** 367-374.

Bolte, S., Brown, S., and Satiat-Jeunemaitre, B. (2004). The N-myristoylated Rab-GTPase m-Rabmc is involved in post-Golgi trafficking events to the lytic vacuole in plant cells. J. Cell Sci. **117,** 943-954.

Costaguta, G., Stefan, C.J., Bensen, E.S., Emr, S.D., and Payne, G.S. (2001). Yeast Gga coat proteins function with clathrin in Golgi to endosome transport. Mol. Biol. Cell. **12,** 1885-1896.

Craddock, C.P., Hunter, P.R., Szakacs, E., Hinz, G., Robinson, D.G., and Frigerio, L. (2008). Lack of a vacuolar sorting receptor leads to non-specific missorting of soluble vacuolar proteins in Arabidopsis seeds. Traffic. **9,** 408-416.

Cullinane, A.R., Schaffer, A.A., and Huizing, M. (2013). The BEACH is hot: A LYST of emerging roles for BEACH-domain containing proteins in human disease. Traffic **14**, 749-766.

de Souza, N., Vallier, L.G., Fares, H., and Greenwald, I. (2007). SEL-2, the C. elegans neurobeachin/LRBA homolog, is a negative regulator of lin-12/Notch activity and affects endosomal traffic in polarized epithelial cells. Development. **134,** 691-702.

Deloche, O., Yeung, B.G., Payne, G.S., and Schekman, R. (2001). Vps10p transport from the trans-Golgi network to the endosome is mediated by clathrin-coated vesicles. Mol. Biol. Cell. **12,** 475-485.

Dereeper, A., Guignon, V., Blanc, G., Audic, S., Buffet, S., Chevenet, F., Dufayard, J.F., Guindon, S., Lefort, V., Lescot, M., Claverie, J.M., and Gascuel, O. (2008). Phylogeny.fr: robust phylogenetic analysis for the non-specialist. Nucleic Acids Res. **36,** W465-469.

Doray, B., Ghosh, P., Griffith, J., Geuze, H.J., and Kornfeld, S. (2002). Cooperation of GGAs and AP-1 in packaging MPRs at the trans-Golgi network. Science. **297,** 1700-1703.

Ebine, K., Inoue, T., Ito, J., Ito, E., Uemura, T., Goh, T., Abe, H., Sato, K., Nakano, A., and Ueda, T. (2014). Plant vacuolar trafficking occurs through distinctly regulated pathways. Curr. Biol. **24,** 1375-1382.

Feraru, E., Paciorek, T., Feraru, M.I., Zwiewka, M., De Groodt, R., De Rycke, R., Kleine-Vehn, J., and Friml, J. (2010). The AP-3 beta adaptin mediates the biogenesis and function of lytic vacuoles in Arabidopsis. Plant Cell. **22,** 2812-2824.

Frigerio, L., Hinz, G., and Robinson, D.G. (2008). Multiple vacuoles in plant cells: rule or exception? Traffic. **9,** 1564-1570.

Frigerio, L., Jolliffe, N.A., Di Cola, A., Felipe, D.H., Paris, N., Neuhaus, J.M., Lord, J.M., Ceriotti, A., and Roberts, L.M. (2001). The internal propeptide of the

ricin precursor carries a sequence-specific determinant for vacuolar sorting. Plant Physiol. **126,** 167-175.

Fuji, K., Shimada, T., Takahashi, H., Tamura, K., Koumoto, Y., Utsumi, S., Nishizawa, K., Maruyama, N., and Hara-Nishimura, I. (2007). Arabidopsis vacuolar sorting mutants (green fluorescent seed) can be identified efficiently by secretion of vacuole-targeted green fluorescent protein in their seeds. Plant Cell. **19,** 597-609.

Ghosh, P., Dahms, N.M., and Kornfeld, S. (2003). Mannose 6-phosphate receptors: new twists in the tale. Nat. Rev. Mol. Cell Biol.. **4,** 202-212.

Hatsugai, N., Iwasaki, S., Tamura, K., Kondo, M., Fuji, K., Ogasawara, K., Nishimura, M., and Hara-Nishimura, I. (2009). A novel membrane fusion-mediated plant immunity against bacterial pathogens. Genes Dev. **23,** 2496-2506.

Heidrich, K., Wirthmueller, L., Tasset, C., Pouzet, C., Deslandes, L., and Parker, J.E. (2011). Arabidopsis EDS1 connects pathogen effector recognition to cell compartment-specific immune responses. Science. **334,** 1401-1404.

Hunter, P.R., Craddock, C.P., Di Benedetto, S., Roberts, L.M., and Frigerio, L. (2007). Fluorescent reporter proteins for the tonoplast and the vacuolar lumen identify a single vacuolar compartment in Arabidopsis cells. Plant Physiol. **145,** 1371-1382.

Introne, W., Boissy, R.E., and Gahl, W.A. (1999). Clinical, molecular, and cell biological aspects of Chediak-Higashi syndrome. Mol. Genet. Metab. **68,** 283-303.

Jogl, G., Shen, Y., Gebauer, D., Li, J., Wiegmann, K., Kashkar, H., Kronke, M., and Tong, L. (2002). Crystal structure of the BEACH domain reveals an unusual fold and extensive association with a novel PH domain. EMBO J. **21,** 4785-4795.

Jolliffe, N.A., Brown, J.C., Neumann, U., Vicre, M., Bachi, A., Hawes, C., Ceriotti, A., Roberts, L.M., and Frigerio, L. (2004). Transport of ricin and 2S albumin precursors to the storage vacuoles of Ricinus communis endosperm involves the Golgi and VSR-like receptors. Plant J. **39,** 821-833.

Khodosh, R., Augsburger, A., Schwarz, T.L., and Garrity, P.A. (2006). Bchs, a BEACH domain protein, antagonizes Rab11 in synapse morphogenesis and other developmental events. Development. **133,** 4655-4665.

Kirsch, T., Paris, N., Butler, J.M., Beevers, L., and Rogers, J.C. (1994). Purification and initial characterization of a potential plant vacuolar targeting receptor. Proc. Nat. Acad. Sci. U S A. **91,** 3403-3407.

Kwak, E., Gerald, N., Larochelle, D.A., Vithalani, K.K., Niswonger, M.L., Maready, M., and De Lozanne, A. (1999). LvsA, a protein related to the mouse beige protein, is required for cytokinesis in Dictyostelium. Mol. Biol. Cell. **10,** 4429-4439.

Kypri, E., Schmauch, C., Maniak, M., and De Lozanne, A. (2007). The BEACH protein LvsB is localized on lysosomes and postlysosomes and limits their fusion with early endosomes. Traffic. **8,** 774-783.

Lemmon, M.A. (2004). Pleckstrin homology domains: not just for phosphoinositides. Biochemical Society Transactions. **32,** 707-711.

Lim, A., and Kraut, R. (2009). The Drosophila BEACH family protein, blue cheese, links lysosomal axon transport with motor neuron degeneration. J.

Neurosci. **29,** 951-963.

Matsuoka, K., and Neuhaus, J.-M. (1999). Cis-elements of protein transport to the plant vacuoles. J. Exp. Bot. **50,** 165-174.

Nakayama, K., and Wakatsuki, S. (2003). The structure and function of GGAs, the traffic controllers at the TGN sorting crossroads. Cell. Struct. Funct. **28,** 431-442.

Neer, E.J., Schmidt, C.J., Nambudripad, R., and Smith, T.F. (1994). The ancient regulatory-protein family of WD-repeat proteins. Nature. **371,** 297-300.

Neuhaus, J.M., and Rogers, J.C. (1998). Sorting of proteins to vacuoles in plant cells. Plant Mol. Biol. **38,** 127-144.

Niihama, M., Takemoto, N., Hashiguchi, Y., Tasaka, M., and Morita, M.T. (2009). ZIP genes encode proteins involved in membrane trafficking of the TGN-PVC/vacuoles. Plant Cell Physiol. **50,** 2057-2068.

Nishizawa, K., Maruyama, N., Satoh, R., Fuchikami, Y., Higasa, T., and Utsumi, S. (2003). A C-terminal sequence of soybean beta-conglycinin alpha' subunit acts as a vacuolar sorting determinant in seed cells. Plant J. **34,** 647-659.

North, H., Baud, S., Debeaujon, I., Dubos, C., Dubreucq, B., Grappin, P., Jullien, M., Lepiniec, L., Marion-Poll, A., Miquel, M., Rajjou, L., Routaboul, J.M., and Caboche, M. (2010). Arabidopsis seed secrets unravelled after a decade of genetic and omics-driven research. Plant J. **61,** 971-981.

Obayashi, T., Nishida, K., Kasahara, K., and Kinoshita, K. (2011). ATTED-II updates: condition-specific gene coexpression to extend coexpression analyses and applications to a broad range of flowering plants. Plant Cell Physiol. **52,** 213-219.

Okita, T.W., and Rogers, J.C. (1996). Compartmentation of proteins in the endomembrane system of plant cells. Annu. Rev. Plant Biol. **47,** 327-350.

Paris, N., Stanley, C.M., Jones, R.L., and Rogers, J.C. (1996). Plant cells contain two functionally distinct vacuolar compartments. Cell. **85,** 563-572.

Park, M., Lee, D., Lee, G.J., and Hwang, I. (2005). AtRMR1 functions as a cargo receptor for protein trafficking to the protein storage vacuole. J. Cell Biol. **170,** 757-767.

Pourcher, M., Santambrogio, M., Thazar, N., Thierry, A.M., Fobis-Loisy, I., Miege, C., Jaillais, Y., and Gaude, T. (2010). Analyses of sorting nexins reveal distinct retromer-subcomplex functions in development and protein sorting in Arabidopsis thaliana. Plant Cell. **22,** 3980-3991.

Rahman, M., Haberman, A., Tracy, C., Ray, S., and Kramer, H. (2012). Drosophila mauve Mutants Reveal a Role of LYST Homologs Late in the Maturation of Phagosomes and Autophagosomes. Traffic. 13, 1680-1692.

Robinson, D.G., Oliviusson, P., and Hinz, G. (2005). Protein sorting to the storage vacuoles of plants: a critical appraisal. Traffic. **6,** 615-625.

Rohrer, J., and Kornfeld, R. (2001). Lysosomal hydrolase mannose 6-phosphate uncovering enzyme resides in the trans-Golgi network. Mol. Biol. Cell. **12,** 1623-1631.

Rossignol, P., Collier, S., Bush, M., Shaw, P., and Doonan, J.H. (2007). Arabidopsis POT1A interacts with TERT-V(I8), an N-terminal splicing variant of telomerase. J. Cell Sci. **120,** 3678-3687.

Saalbach, G., Rosso, M., and Schumann, U. (1996). The vacuolar targeting signal of the 2S albumin from Brazil nut resides at the C terminus and involves

the C-terminal propeptide as an essential element. Plant Physiol. **112,** 975-985.

Saedler, R., Jakoby, M., Marin, B., Galiana-Jaime, E., and Hulskamp, M. (2009). The cell morphogenesis gene SPIRRIG in Arabidopsis encodes a WD/BEACH domain protein. Plant J. **59,** 612-621.

Sanmartin, M., Ordonez, A., Sohn, E.J., Robert, S., Sanchez-Serrano, J.J., Surpin, M.A., Raikhel, N.V., and Rojo, E. (2007). Divergent functions of VTI12 and VTI11 in trafficking to storage and lytic vacuoles in Arabidopsis. Proc. Nat. Acad. Sci. U S A. **104,** 3645-3650.

Shiflett, S.L., Vaughn, M.B., Huynh, D., Kaplan, J., and Ward, D.M. (2004). Bph1p, the Saccharomyces cerevisiae homologue of CHS1/beige, functions in cell wall formation and protein sorting. Traffic. **5,** 700-710.

Shimada, T., Fuji, K., Tamura, K., Kondo, M., Nishimura, M., and Hara-Nishimura, I. (2003). Vacuolar sorting receptor for seed storage proteins in Arabidopsis thaliana. Proc. Nat. Acad. Sci. U S A. **100,** 16095-16100.

Singh, M.K., Kruger, F., Beckmann, H., Brumm, S., Vermeer, J.E., Munnik, T., Mayer, U., Stierhof, Y.D., Grefen, C., Schumacher, K., and Jurgens, G. (2014). Protein delivery to vacuole requires SAND protein-dependent Rab GTPase conversion for MVB-vacuole fusion. Curr. Biol.**24,** 1383-1389.

Su, Y., Balice-Gordon, R.J., Hess, D.M., Landsman, D.S., Minarcik, J., Golden, J., Hurwitz, I., Liebhaber, S.A., and Cooke, N.E. (2004). Neurobeachin is essential for neuromuscular synaptic transmission. J. Neurosci. **24,** 3627-3636.

Tabata, R., Kamiya, T., Shigenobu, S., Yamaguchi, K., Yamada, M., Hasebe, M., Fujiwara, T., and Sawa, S. (2013). Identification of an EMS-induced causal mutation in a gene required for boron-mediated root development by low-coverage genome re-sequencing in Arabidopsis. Plant Signal. Behav. **8(1)**, e22534.

Teh, O.K., and Hofius, D. (2014). Membrane trafficking and autophagy in pathogen-triggered cell death and immunity. J. Exp. Bot. **65,** 1297-1312.

Teh, O.K., Shimono, Y., Shirakawa, M., Fukao, Y., Tamura, K., Shimada, T., and Hara-Nishimura, I. (2013). The AP-1 μ adaptin is required for KNOLLE localization at the cell plate to mediate cytokinesis in *Arabidopsis*. Plant Cell Physiol. **54**, 838-847.

Uemura, T., Kim, H., Saito, C., Ebine, K., Ueda, T., Schulze-Lefert, P., and Nakano, A. (2012). Qa-SNAREs localized to the trans-Golgi network regulate multiple transport pathways and extracellular disease resistance in plants. Proc. Nat. Acad. Sci. U S A. **109,** 1784-1789.

Wang, X., Herberg, F.W., Laue, M.M., Wullner, C., Hu, B., Petrasch-Parwez, E., and Kilimann, M.W. (2000). Neurobeachin: A protein kinase A-anchoring, beige/Chediak-higashi protein homolog implicated in neuronal membrane traffic. J. Neurosci. **20,** 8551-8565.

Yano, D., Sato, M., Saito, C., Sato, M.H., Morita, M.T., and Tasaka, M. (2003). A SNARE complex containing SGR3/AtVAM3 and ZIG/VTI11 in gravity-sensing cells is important for Arabidopsis shoot gravitropism. Proc. Nat. Acad. Sci. U S A. **100,** 8589-8594.

Yao, L., Kawakami, Y., and Kawakami, T. (1994). The pleckstrin homology domain

of Bruton tyrosine kinase interacts with protein kinase C. Proc. Nat. Acad. Sci. U S A. **91,** 9175-9179.

Zheng, H., Kunst, L., Hawes, C., and Moore, I. (2004). A GFP-based assay reveals a role for RHD3 in transport between the endoplasmic reticulum and Golgi apparatus. Plant J. **37,** 398-414.

Zouhar, J., Munoz, A., and Rojo, E. (2010). Functional specialization within the vacuolar sorting receptor family: VSR1, VSR3 and VSR4 sort vacuolar storage cargo in seeds and vegetative tissues. Plant J. **64,** 577-588.

Zwiewka, M., Feraru, E., Moller, B., Hwang, I., Feraru, M.I., Kleine-Vehn, J., Weijers, D., and Friml, J. (2011). The AP-3 adaptor complex is required for vacuolar function in Arabidopsis. Cell Research. **21,** 1711-1722.

Figure 1

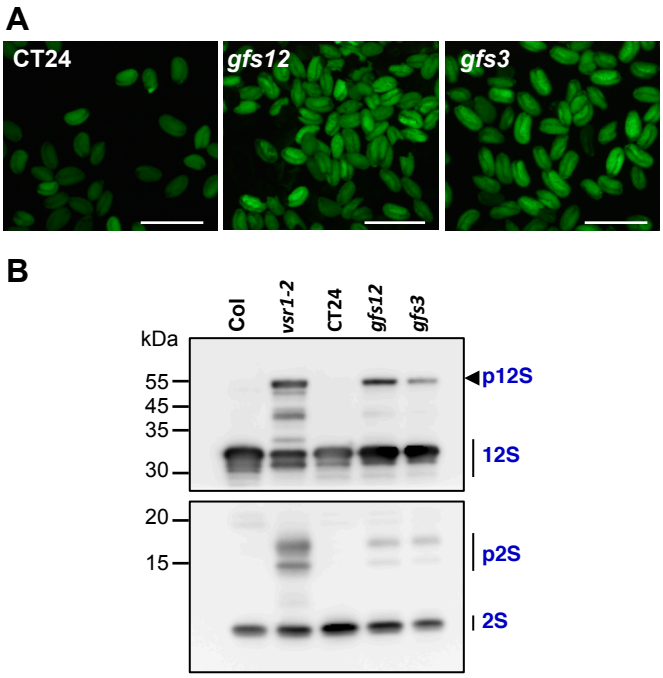

Figure 1. *gfs12* and *gfs3* Are Vacuolar Protein Trafficking Mutants.
(**A**) Comparison of fluorescence of *gfs3*, *gfs12* and parental CT24 seeds expressed a PSV-targeted GFP. Imaging parameters were the same for each panel. Bars=1cm.
(**B**) 12S globulin and 2S albumin immunoblot of *gfs12* and *gfs3*. Storage protein analysis of *gfs12* and *gfs3* showed that they accumulated unprocessed 12S globulin precursors (p12S) and trace amount of unprocessed 2S albumin precursors (p2S), unlike the *vsr1-2* which massively accumulates both type of precursors.

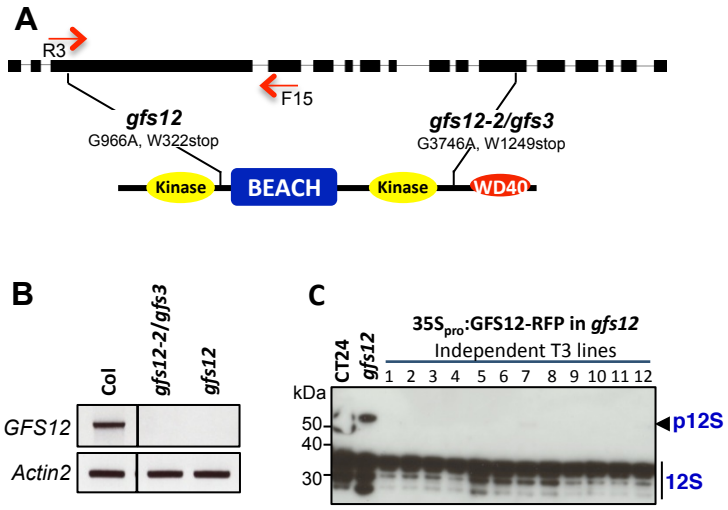

Figure 2. *gfs12* and *gfs3* Are alleles of a BEACH-Domain Locus.
(**A**) (Top) Schematic representation of locus At5g18525. The locus is now renamed as *GFS12*. Exons and introns are indicated by boxes and lines respectively. Red arrows indicate primers used in RT-PCR. Locations of mutations in *gfs12* (G966A, W322stop) and *gfs12-2* (G3746A, W1249stop) are shown. (Bottom) Schematic representation of the corresponding *GFS12* protein structure. Kinase domains are marked by yellow ovals, blue rectangle represents BEACH domain and red oval indicates WD40 repeats.
(**B**) *gfs12* and *gfs12-2* are knock-out alleles of *GFS12*. RT-PCR of *GFS12* transcript in *gfs12* and *gfs12-2/gfs3*. *Actin2* was used as loading control. Primers used (F15 and R3) are indicated by red arrows in (**A**). Cycle numbers for GFS12 and Actin2 are 35 and 28 respectively.
(**C**) Abnormal accumulation of 12S globulin precursor (p12S) is complemented by a RFP-fusion protein of GFS12. Numbers on top indicate independent T3 lines of *gfs12* transformed with GFS12-RFP under 35S promoter.

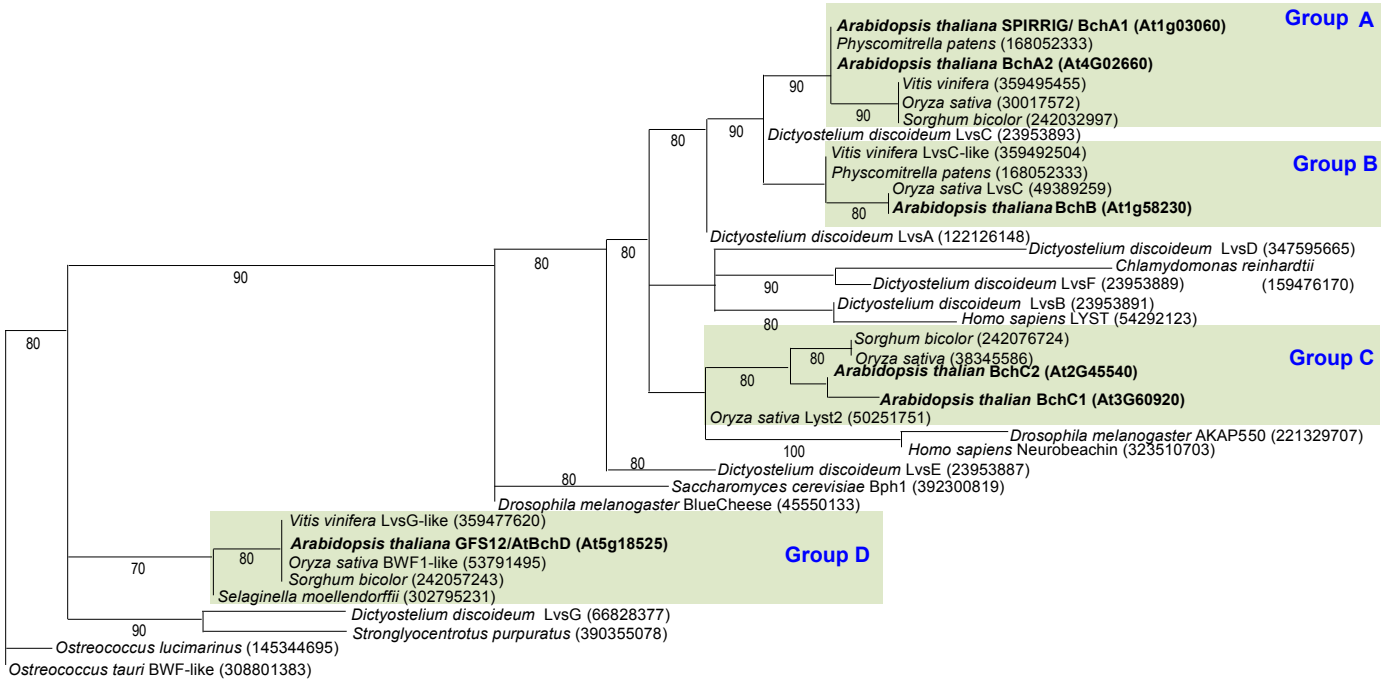

Figure 3. Phylogenetic Tree of BEACH-Domain Proteins Constructed by the Neighbor-Joining Method with Phylogeny.

Amino acid sequences of the BEACH domains (Table S1) from dicot, monocot, animals, slime mould, moss, green alga and lycophyte were edited, aligned and analyzed using neighbour-joining method (Dereeper et al., 2008). GenBank accession numbers (in the case of *Arabidopsis*, AGI codes) are shown in parentheses. Green boxes indicate plant-specific BEACH homologs. Numbers at the branches indicate bootstrap values.

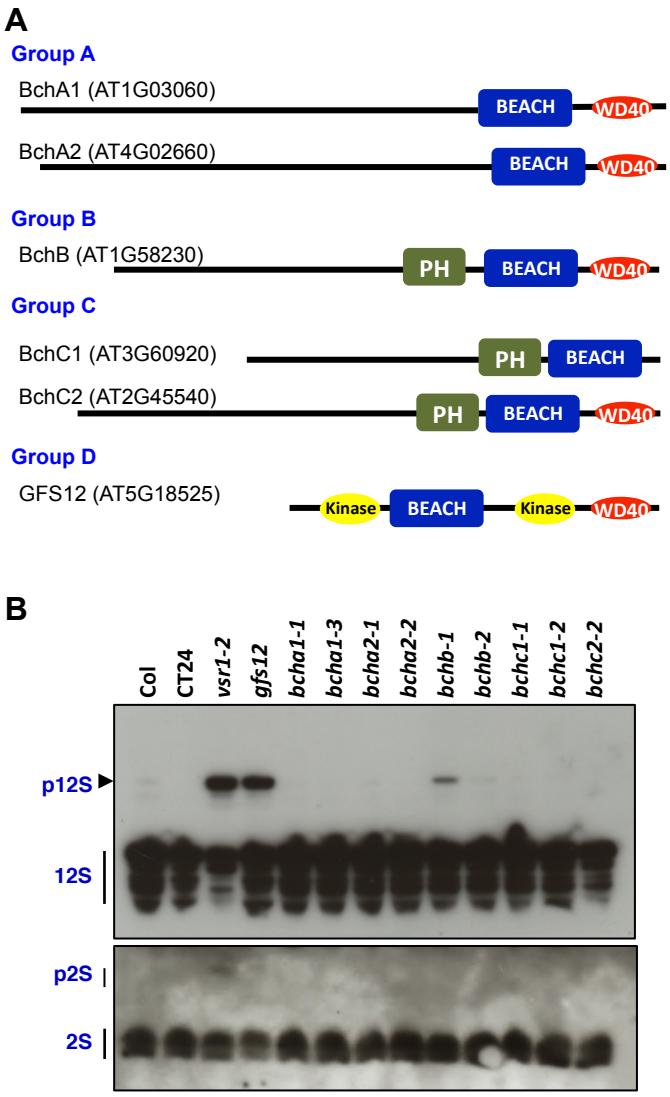

Figure 4. GFS12 Has Overlapping Functions with BchB in Vacuolar Protein Trafficking.
(**A**) Schematic representation of four groups of BEACH-domain protein in *Arabidopsis*. Solid line and red-filled oval represent the highly variable regions and WD40 repeat domain respectively. PH is pleckstrin homology domains. GFS12 is the only BEACH protein that possesses kinase domains. Note that WD40 repeats are missing from BchC1.
(**B**) Anti-12S and anti-2S immunoblots of BEACH homolog knock-out or knock-down mutants showing that only *gfs12* and *bchb-1* specifically accumulated 12S globulin precursor (p12S) but not 2S albumin precursors (p2S).

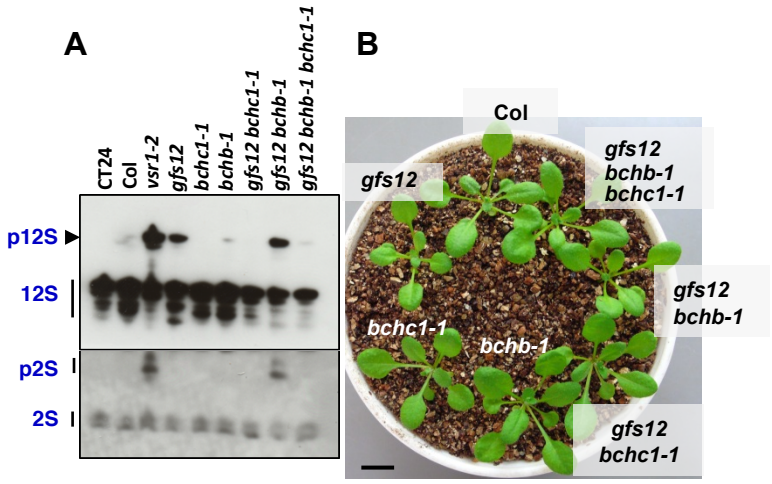

Figure 5. Epistatic and Synergistic Genetic Interactions between GFS12 and BEACH Homologs.

(**A**) Anti-12S and anti-2S immunoblots of BEACH-domain double mutants. GFS12 showed synergistic genetic interactions with *BchB* as double mutant *gfs12 bchb-1* accumulated significant amount of 12S globulin precursor (p12S) compared to single mutants *gfs12* and *bchb-1*. The 2S albumin precursors (p2S) also began to accumulate in *gfs12 bchb-1*. The *bchc1-1* mutation is epistatic to *gfs12* since no p12S can be detected in double mutant *gfs12 bchc1-1*. Triple mutant *gfs12 bchb-1 bchc1-1* showed reduced p12S accumulation compared to double mutant *gfs12 bchb-1*. Note that p2S accumulation in *gfs12 bchb-1* was also suppressed when *bchc1-1* mutation was introduced.

(**B**) GFS12 and BEACH homologs are not important for *Arabidopsis* general growth. All mutant combination showed normal growth compared to wild type control. Bar=1cm.

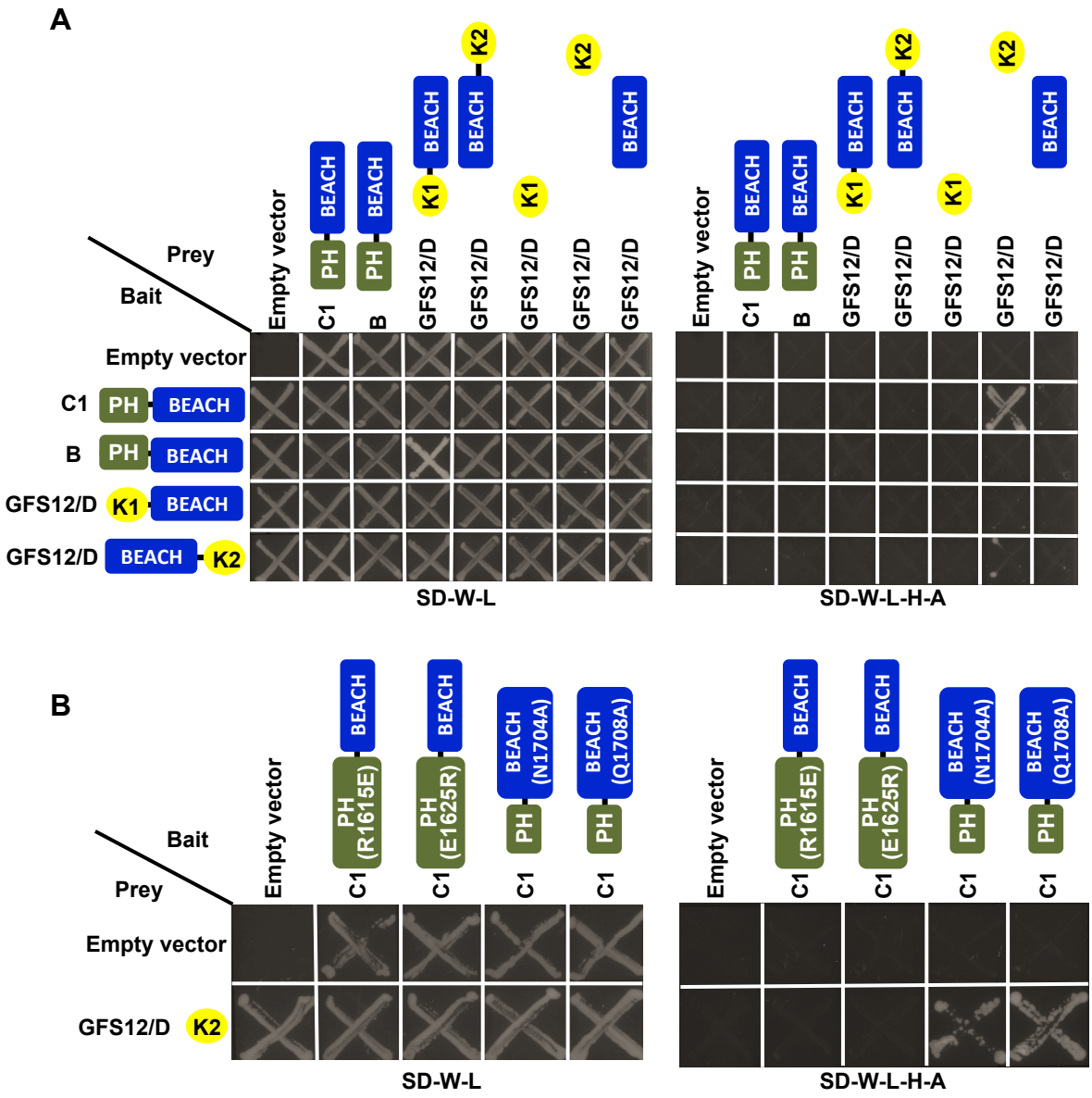

Figure 6. Yeast-Two-Hybrid Assay of GFS12, BchB and BchC1.
(**A**) The GFS12/BchD Kinase I-BEACH (GFS12/D K1-Bch), BEACH-Kinase domain II (GFS12/D Bch-K2), Kinase domain I only (GFS12/D K1), Kinase domain II only (GFS12/D K2), BEACH domain only (GFS12/D Bch), BchC1 PH-BEACH domain (C1 PH-Bch) and BchB PH-BEACH domain (B PH-Bch) were cloned in pDEST-GADT7. These constructs were tested for interaction against the bait constructs in pDEST-GBKT7 which includes C1 PH-Bch, B PH-Bch, GFS12/D K1-Bch and GFS12/D Bch-K2. Yeast strains harbouring the prey and bait constructs were selected on single dropout (SD) media minus tryptophan and leucine (SD-W-L). When these yeast strains were plated on SD media without essential amino acids histidine and adenine (SD-W-L-H-A), only yeast strain harbouring pDEST-GADT7:GFS12/D K2 and pDEST-GBKT7:C1 PH-Bch grew.
(B) Site directed mutagenesis in the BchC1 PH domain (R1625E and E1625R) disrupted the BchC1 interaction with GFS12 Kinase II domain. On the contrary, mutations (N1704A and Q1708A) in the BchC1 BEACH domain have no effect on the BchC1-GFS12 Kinase II interaction.

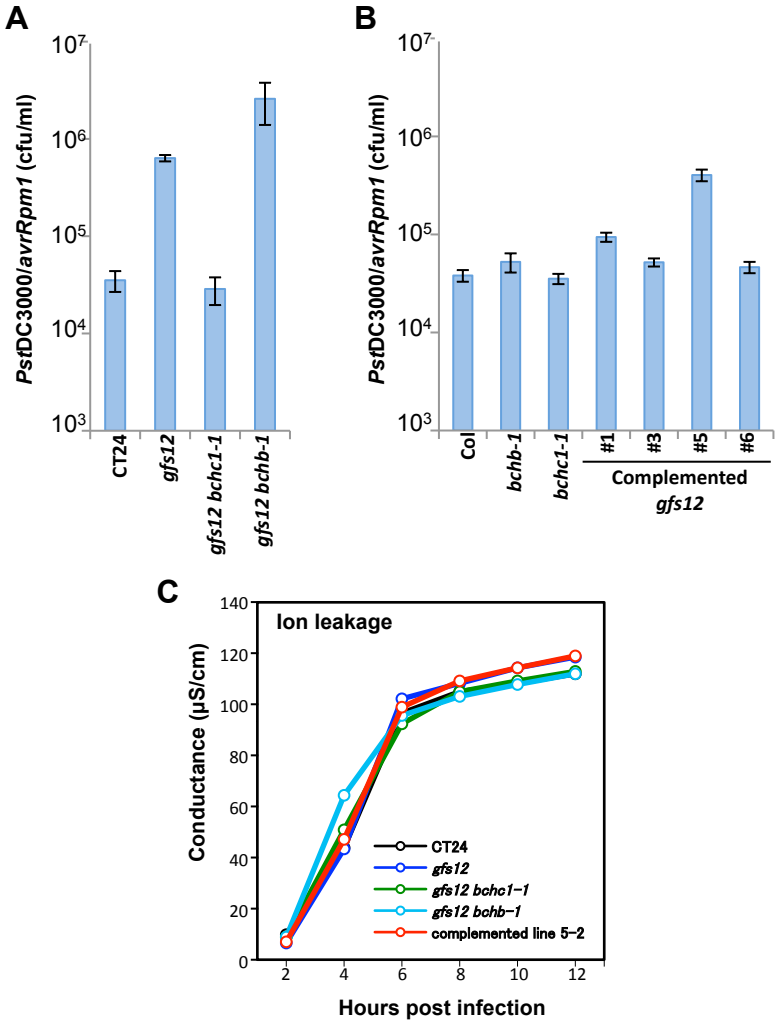

Figure 7. Effector Triggered Immunity Is Compromised in *gfs12*.
(**A, B**) Five-week-old plants of various genetic backgrounds were infiltrated with *Pst*DC3000/*avrRpm1*. Bacterial growth titer was assayed 3 days later. Error bars=standard errors.
(**C**) Ion leakage assay of the control CT24 parental plants, *gfs12*, *gfs12 bchc1-1*, *gfs12 bchb-1* and complemented *gfs12* plants. They were infected with *Pst*DC3000/ *avrRpm1*. The ion leakage from dying and dead cells was measured by conductance.

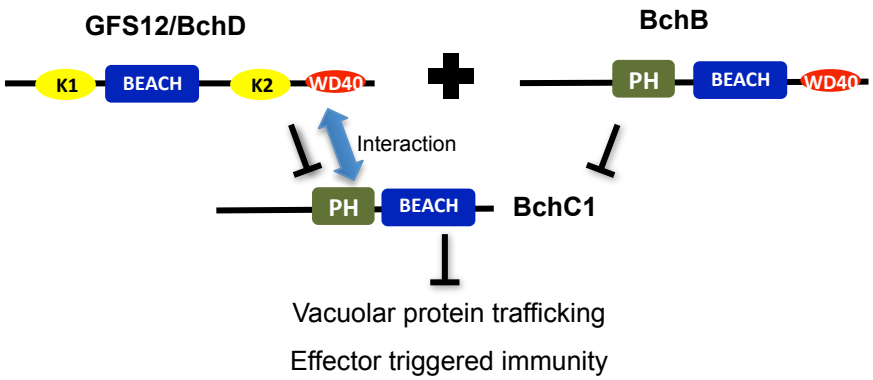

Figure 8. Working Model on the BEACH Protein Cascade Action in Regulating Storage Protein Trafficking and Plant Immunity Response.
We propose that GFS12, BchB and BchC1 acts in a cascading manner to regulate storage protein trafficking. GFS12 interacts with BchC1 via the PH domain. The interaction inactivates BchC1 which is a negative regulator for the PSV trafficking and plant immunity response. Note that GFS12 has a predominant role over BchB in BchC1 inhibition.

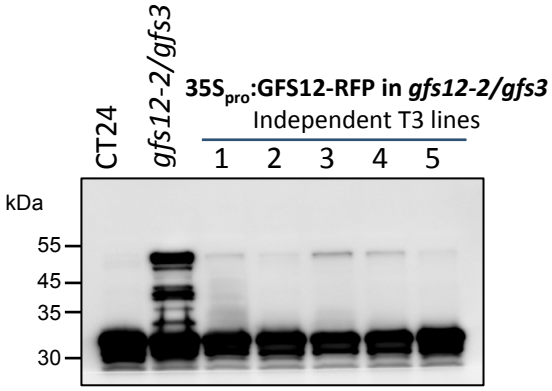

Supplemental Figure 1. Abnormal accumulation of 12S globulin precursor (p12S) in *gfs12-2/gfs3* is complemented by a RFP-fusion protein of GFS12. Numbers on top indicate independent T3 lines of *gfs12-2/gfs3* transformed with GFS12-RFP under 35S promoter.

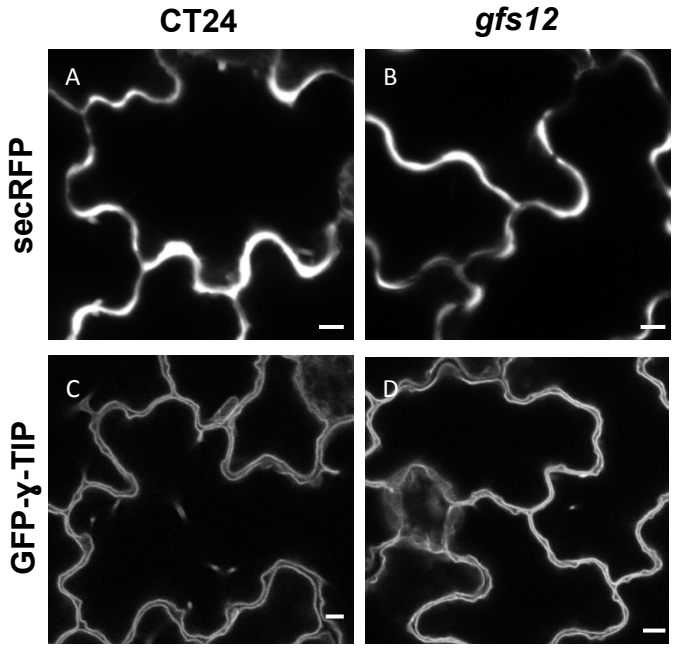

Supplemental Figure 2. Secretory and lytic vacuole trafficking pathways were unaffected in *gfs12*. CLSM analysis of *gfs12* stably expressing different markers in cotyledon. Bars=5µm. (**A, B**) Expression of the secretory marker secRFP in CT24 (A) and *gfs12* (B) showed that the secretion in *gfs12* was unaffected as RFP signal was detected in the apoplastic regions. (**C, D**) Expression of vacuolar membrane protein GFP-ɣ-TIP in CT24 (C) and *gfs12* (D) showed that the membrane protein was correctly targeted to the lytic vacuole.

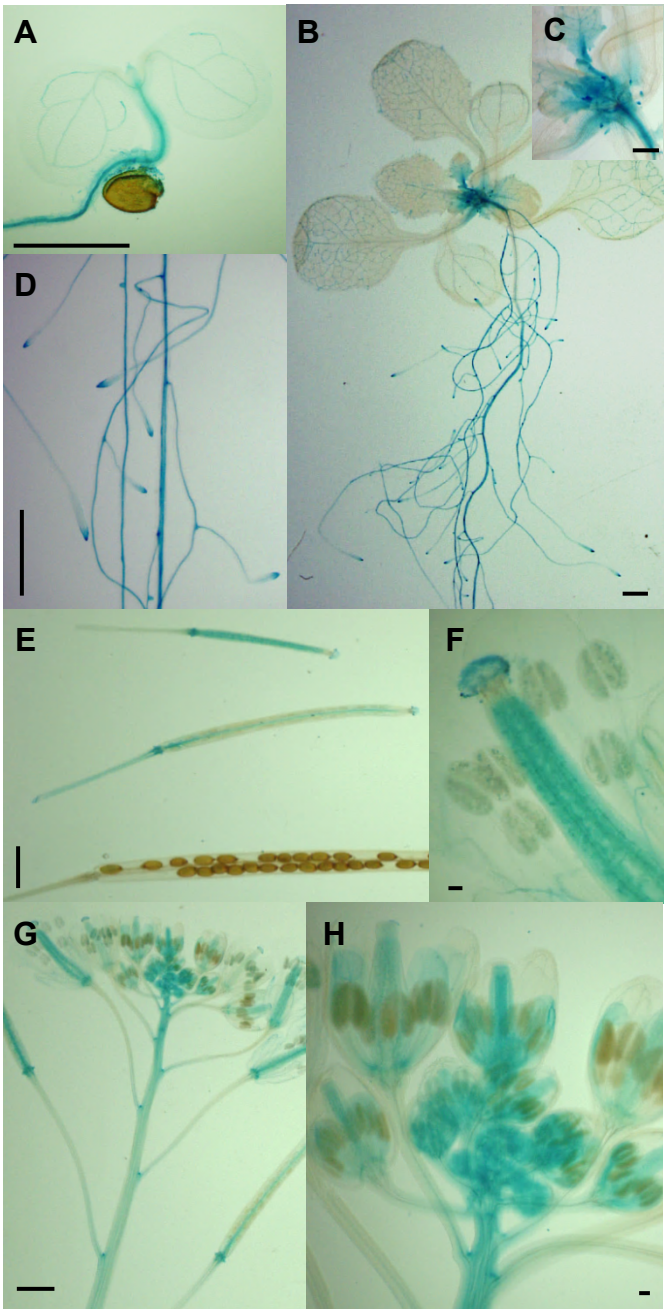

Supplemental Figure 3. *GFS12* expressed weakly in specific tissues. GFS12 expression pattern as revealed by the GFS12 promoter GUS fusion. GFS12 expresses weakly from early stage of the seedling development (**A**) with distinct root tip (**D**) and vein tissues (**B**) staining pattern. High expression was also found in the apical meristem (**B, C**). GFS12 expression was relatively weak at the reproductive stage (**E-H**). In developing siliques, the GFS12 expression diminished as the seeds developed (**E**). Weak expression of GFS12 was also detected in the stigma and style (F), receptacles (**G**) and young flower buds (**H**). Bars, 0.1cm.

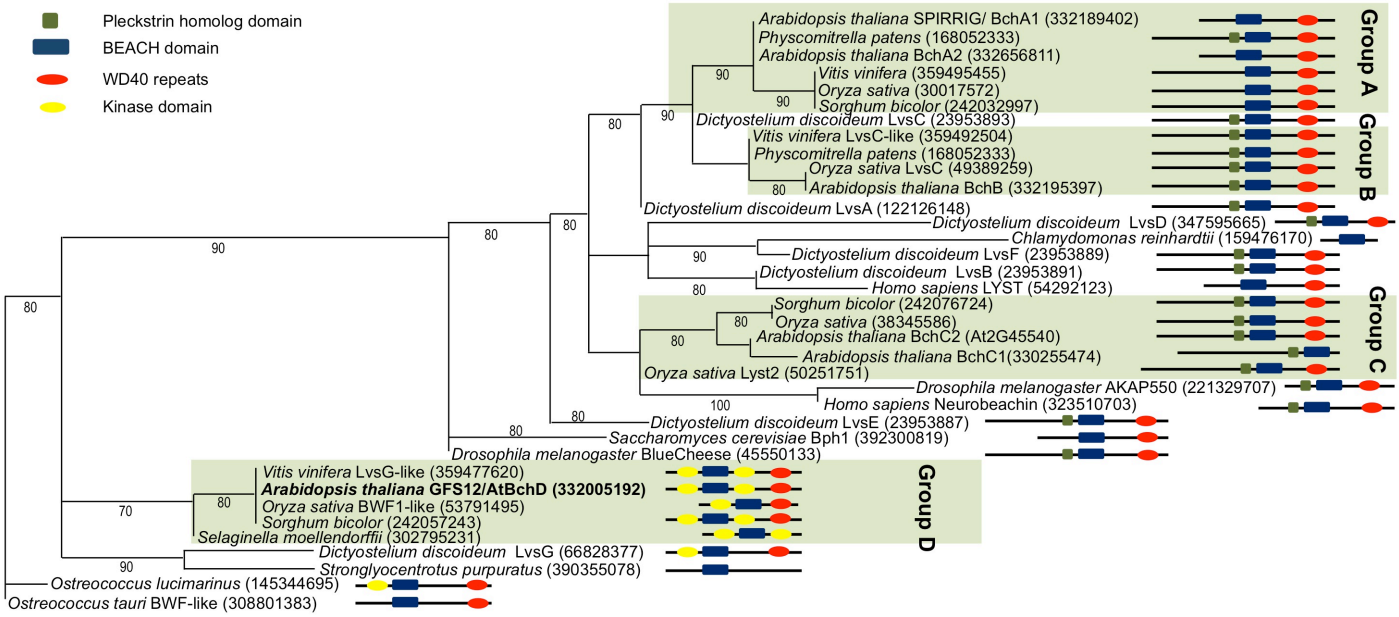

Supplemental Figure 4. Schematic representations of the BEACH protein structure. Kinase domains are marked by yellow ovals, blue and green rectangles represent BEACH and PH domains respectively and red oval indicates WD40 repeats. Length of proteins is not drawn to scale.

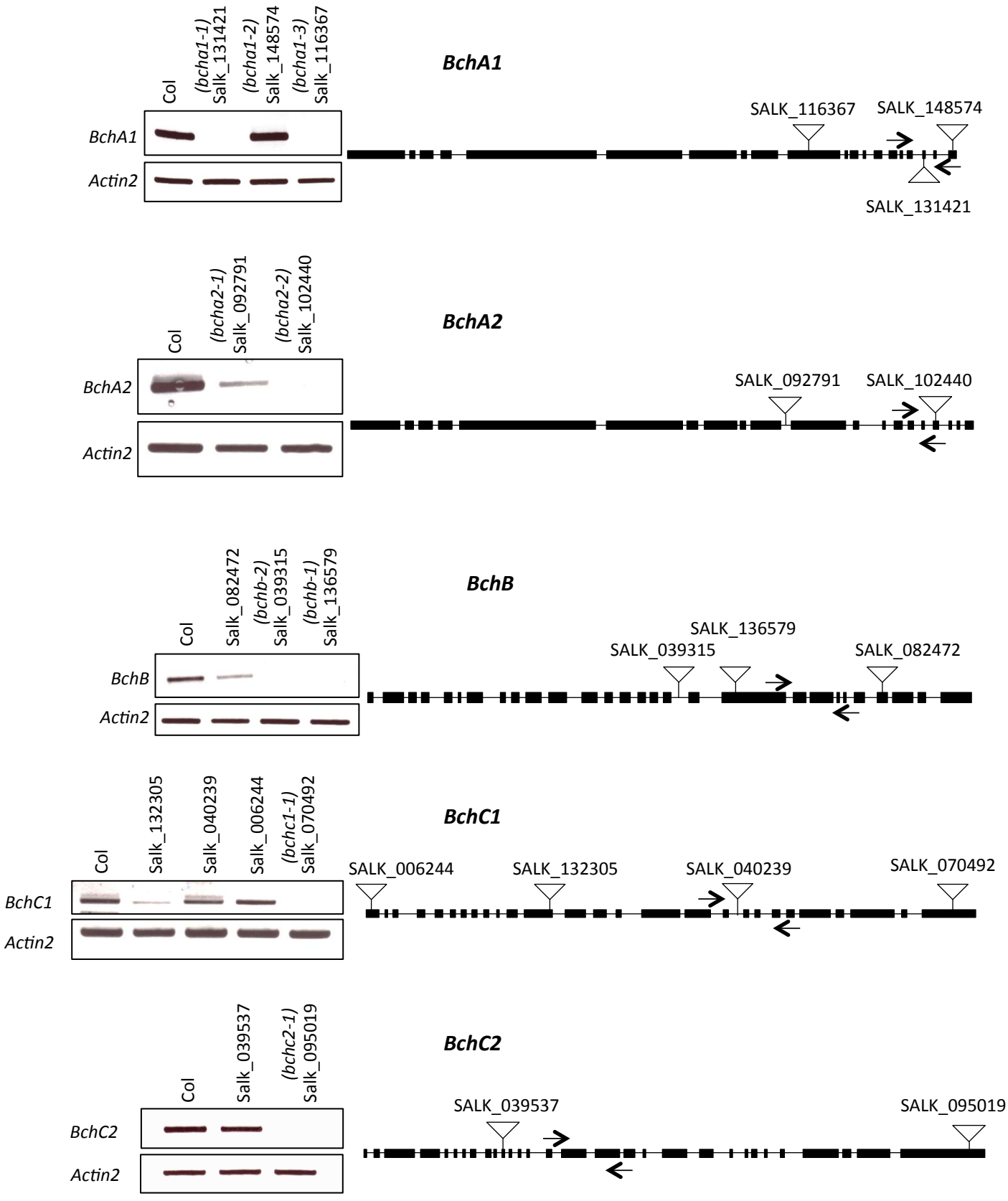

Supplemental Figure 5. Semi quantitative RT-PCR to isolate knock-out and knock-down alleles of BEACH-domain T-DNA mutants. Schematic representation of the T-DNA insertion (inverted triangles) in the BEACH-domain containing genes are indicated on the right and the semi-quantitative RT-PCR analyses of the respective mutant alleles are on the left. *Actin2* was used as loading control in all cases. Darkened rectangle boxes represent exons and introns are indicated by joining lines. Primers used in the semi-quantitative RT-PCR were indicated by arrows.

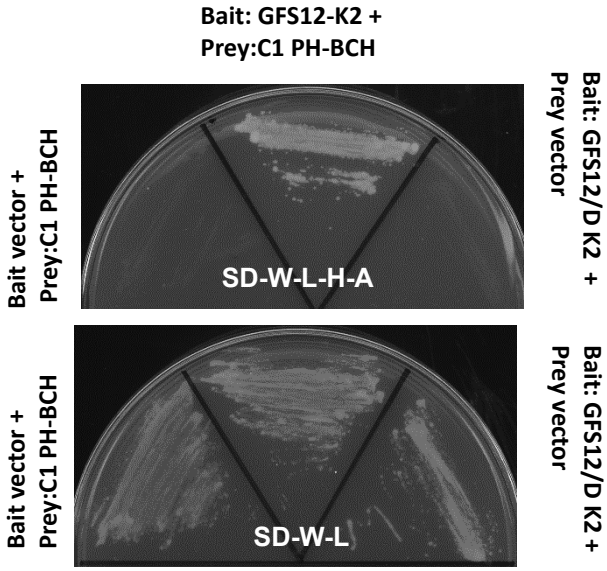

Supplemental Figure 6. Yeast-two-hybrid assay of GFS12 and BchC1. KII domain of GFS12 and PH-BCH domain of BchC1 were expressed in the bait (pDEST-GBDKT7) and prey vectors (pDEST-GADT7) respectively and grown on either SD-W-L media (bottom) or SD-W-L-H-A media (top). Self-activation negative control was also included. Only yeast strain harbouring the pDEST-GBDKT7: GFS12/D K2 and pDEST-GADT7: C1 PH-BCH grew on SD-W-L-H-A media.

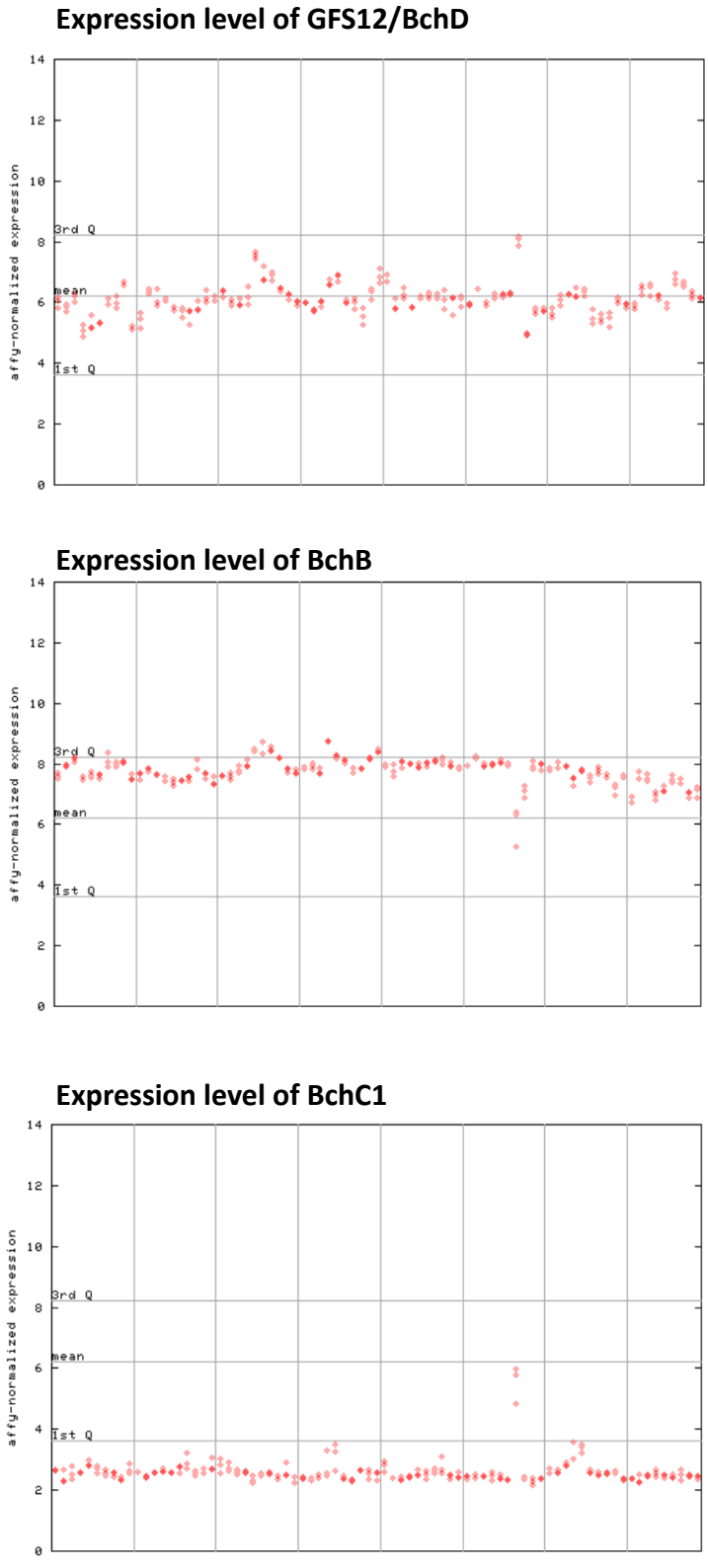

Supplemental Figure 7. Expression levels of *GFS12*/*BchD*, *BchB* and *BchC1* as indicated on the ATTED-II.

Supplemental Table 1. Collection of BEACH-domain amino acid sequences.

Organism	Homolog	GeneBank accession	BEACH-domain amino acid sequence
Arabidopsis thaliana	SPIRRIG/At1g03060	332189402	K2965 to R3244
Arabidopsis thaliana	BchB/At1g58230	332195397	D1948 to Y2586
Arabidopsis thaliana	BchC2/At2g45540	330255474	M2232 to R2509
Arabidopsis thaliana	BchC1/At3g60920	332646606	W1422 to L1828
Arabidopsis thaliana	BchA2/At4g02660	332656811	W2824 to S2254
Arabidopsis thaliana	GFS12/BchD/At5g18525	332005192	S329 to R580
Homo sapiens	Nuerobeachin	323510703	T79 to R356
Homo sapiens	LYST	54292123	T3132 to R3422
Dictyostelium discoideum	LvsA	122126148	T2984 to R3270
Dictyostelium discoideum	LvsB	23953891	T3018 to K3297
Dictyostelium discoideum	LvsC	23953893	T1859 to R2137
Dictyostelium discoideum	LvsD	347595665	T1754 to R2032
Dictyostelium discoideum	LvsE	23953887	T1253 to R1532
Dictyostelium discoideum	LvsF	23953889	K407 to H698
Dictyostelium discoideum	LvsG	66828377	M475 to N760
Drosophila melanogaster	BlueCheese	45550133	T2637 to K2918
Drosophila melanogaster	AKAP550	221329707	T2893 to R3170
Oryza sativa	Os04g46894	38345586	T2160 to G2377
Oryza sativa	LvsC	49389259	N2034 to R2302
Oryza sativa	Lyst2	50251751	F2158 to R2407
Oryza sativa	Os03g53280.1	30017572	R2978 to R3256
Oryza sativa	BWF1-like	53791495	S156 to R407
Sorghum bicolor	01g008410	242032997	K2902 to R3181
Sorghum bicolor	06g024850	242076724	M139 to R416
Sorghum bicolor	03g013240	242057243	K280 to R511
Saccharomyces cerevisiae	Bph1p	392300819	K835 to K1116
Ostreococcus tauri	BWF-like	308801383	A16 to R251
Stronglyocentrotus purpuratus		390355078	M346 to R589
Ostreococcus lucimarinus		145344695	T148 to R386
Physcomitrella patens		168052333	Q1921 to V2151
Physcomitrella patens		168024898	R3099 to V3330
Selaginella moellendorffii		302795231	V106 to R348
Vitis vinifera	LvsG-like	359477620	S348 to P583
Vitis vinifera	LvsC-like	359492504	E2091 to I2326
Vitis vinifera		359495455	R2670 to R2948
Chlamydomonas reinhardtii		159476170	W212 to A425

Supplemental Table 2. DNA sequence of primers used in the semi quantitative RT-PCR of BEACH-domain T-DNA mutants and yeast-two-hybrid assay.

Primer	Experiment	Sequence
At5g18525-F15	RT-PCR	5’ tgagaaatacggagagtccaa 3’
At5g18525-R3	RT-PCR	5’ tcctttgtcttcttcttgggttac 3’
At1g03060-F	RT-PCR	5' tcctgtatttccgtgggttc 3'
At1g03060-R	RT-PCR	5' cacccagatcaaggctgaat 3'
At4g02660-F	RT-PCR	5' gggagatcagcaatttccaa 3'
At4g02660-R	RT-PCR	5' gcttttcacccaaatcaagg 3'
At1g58230-F	RT-PCR	5' gctggttggttggcagttat 3'
At1g58230-R	RT-PCR	5' cctgcaagggtgttgagaat 3'
At3g60920-F	RT-PCR	5' ttctggcactggtcatcttg 3'
At3g60920-R	RT-PCR	5' agaagacatcagccaacttcg 3'
At2g45540-F	RT-PCR	5' gcagcagcagattatgacga 3'
At2g45540-R	RT-PCR	5' acattggccaactacgatcc 3'
60920-PH-Bch-F	Yeast-2-hybrid	5’ aaccaattcagtcgactggaaactggattctatggaaa3’
60920-PH-Bch-R	Yeast-2-hybrid	5’aagctgggtctagatatcctcacaactccttcacattattcata3’
58230-PH-Bch-F	Yeast-2-hybrid	5’aaccaattcagtcgaccacagaagatggaaaatagggaag3’
58230-PH-Bch-R	Yeast-2-hybrid	5’aagctgggtctagatatcctcaataaacaagaagggctccat3’
18525-K1-Bch-F	Yeast-2-hybrid	5’aaccaattcagtcgacgaggaaaaaagcaagcttcgatgt3’
18525-K1-Bch-R	Yeast-2-hybrid	5’aagctgggtctagatatcctcagcgcaccggatgaggccgaaa3’
18525-Bch-K2-F	Yeast-2-hybrid	5’aaccaattcagtcgacgataaatggtggaagggagagcta3’
18525-Bch-K2-R	Yeast-2-hybrid	5’aagctgggtctagatatcctcagaaatacggagagtccaaaaga3’
18525-KI-F	Yeast-2-hybrid	5’aaccaattcagtcgacgaggaaaaaagcaagcttcgat3’
18525-KI-R	Yeast-2-hybrid	5’aagctgggtctagatatccaggtttgctatagatcgttaa3’
18525-Bch-F	Yeast-2-hybrid	5’aaccaattcagtcgacgataaatggtggaagggagag3’
18525-Bch-R	Yeast-2-hybrid	5’aagctgggtctagatatccgcgcaccggatgaggccga3’
18525-K2-F	Yeast-2-hybrid	5’aaccaattcagtcgacgacattgctggggatatttt3’
18525-K2-R	Yeast-2-hybrid	5’aagctgggtctagatatccgaaatacggagagtccaa3’
R1615E-F	Yeast-2-hybrid	5’tatagcgaacgatatctactgaagaag3’
R1615-R	Yeast-2-hybrid	5’atatcgttcgctataaatctgaagaga3’
E1625-F	Yeast-2-hybrid	5’gctcttagactatttatggtggatcgc3’
E1625-R	Yeast-2-hybrid	5’aaatagtctaagagcactcttcttcag3’
N1704A-F	Yeast-2-hybrid	5’agttatgctgacatcactcagtatcct3’
N1704A-R	Yeast-2-hybrid	5’gatgtcagcataactacgcccagccaa3’
Q1708A-F	Yeast-2-hybrid	5’atcactgcttatcctattttcccatgg3’
Q1708A-R	Yeast-2-hybrid	5’aggataagcagtgatgtcattataact3’